Title
SENSITIVITY OF SYNCHRONIZED MAMMALIAN CELLS TO HIGH LET RADIATION

Author
Bird, Richard Putnam.

Publication Date
1972-06-01

SENSITIVITY OF SYNCHRONIZED MAMMALIAN CELLS TO HIGH LET RADIATION

Richard Putnam Bird
(Ph. D. Thesis)

June 1972

AEC Contract No. W-7405-eng-48

LBL-958

DISCLAIMER

SENSITIVITY OF SYNCHRONIZED MAMMALIAN CELLS TO HIGH LET RADIATION

Contents

ABSTRACT

Cultured Chinese hamster cells (V79) were irradiated with 145 kVp x-rays and with high linear energy transfer (LET) radiations at different times in their synchronized cell cycle. The radiation effect scored was killing defined by colony-forming ability in a six-day growth period. The high LET radiations used were accelerated ions of ^{4}He, ^{12}C, ^{20}Ne, and ^{40}A with energies near that of the full energy available at the Berkeley HILAC (10 Mev/a.m.u.). The range of LET values was from about 2 keV/micron to 2000 keV/micron of unit density matter. In addition, asynchronous populations were irradiated with the above accelerated ions and with ^{10}B ions from the HILAC.

Synchronized cultures were obtained by mitotic selection using a mechanical shaker. The degree of synchrony was primarily determined by autoradiographs of pulse-labeled (^{3}H-TdR) cultures and was found to vary from 0.5 to 0.8 in labeling index. Measurements of the cell nucleus cross-section were made also at different times after synchronization.

With low LET radiations, the synchronized cultures exhibited a variation in the survival depending on the cell-cycle time of irradiation, as observed by others. The magnitude of this variation was found to be LET-dependent, decreasing with increasing LET until there was no measurable survival variation (or age-response) when radiations with LET values of 200 keV/micron and higher were used.

The inactivation cross-sections determined for carbon, neon, and argon ion irradiation were 47, 71, and 98 $(microns)^2$, respectively, invariant to cell-cycle time. The cross-section measured for the cell nucleus increased from about 50 to 70 $(microns)^2$ for the usual cell-cycle times of irradiation. Comparison of inactivation cross-sections with the cross-sections of the nucleus indicates that the whole nucleus is not uniformly sensitive at all cell-cycle times. The age-response dependence on LET can be interpreted that the same radiation damage site is involved for low and high LET radiation. The possible application of the results to radiation therapy is discussed.

I. INTRODUCTION

A. Radiation Biology and Radiation Therapy

The association of radiation biology and radiation therapy began early after the discovery of radiation. In 1906, Bergonié and Tribondeau (9) enunciated their "law" which noted that different kinds of cells in tissue were effected to a different degree when irradiated with x-rays. Their "law" related the differences in radiosensitivity to cellular differences in biological activity and they suggested that, in considering radiation for therapy, the relative sensitivity of normal and diseased tissues would be of critical importance. The association of radiobiology and radiation therapy has continued (see review, Ref. 34) with the development of quantitative measurements, especially with the development of techniques for quantitative culturing of mammalian cells.

One tool of radiation biology that is of potential interest for radiation therapy is heavy charged particles. These radiations, with a high LET* value (that is, densely ionizing along the particle track) have been used in numerous biological studies including their effects on cultured mammalian cells (16,7,70,63). Heavy charged particles have been proposed for radiation therapy (69) and radiations such as fast neutrons and negative pi-mesons have been suggested also for radiation therapy (3,26). These latter radiations produce a substantial part of their ionizations along densely ionizing tracks of secondary particles and the biological effect of this component of the radiation dose can be more easily studied directly with heavy charged particles.

With cultured proliferating mammalian cells, the most commonly studied radiation effect is on the ability of the cells to reproduce indefinitely. Radiation survivors are those capable of

---

*LET (linear energy transfer) is used according to the definition of Zirkle and Tobias (83) as the total rate of energy deposition along the charged particle track, often designated LET_{∞}.

forming a colony of cells that reflects unlimited proliferative capacity. This definition has had wide use in quantitative radiation biology and is reasonable in experiments related to radiation therapy.

Cultured proliferating mammalian cells significantly simplify experimental investigations pertinent to radiation therapy. This is justified:

(a) by the generally successful explanation, based on individual cell killing, of radiation effects in pathological studies of multicellular organisms, and

(b) by the similar x-ray doses observed for killing both culture cells and tumour cells (41).

The similarity in dose-response of cultured and tumour cells may be related in a simple way such as that described by Bergonié and Tribondeau (whose most sensitive experimental cells were rapidly proliferating germinal cells) but there may be important differences as well. At present, the testing of very high LET radiations for therapy is limited to small dimensions (such as those found in monolayers of cultured cells) due to the short penetrations of existing beams of such radiations.

Most of the mammalian cell studies using high LET radiations have been made with exponentially growing cultures (16,7,70,63) which therefore contain a mixture of cells of different physiological states. A variety of synchronizing techniques (see review, Ref. 59) have been used in radiation biology studies with x-rays and other radiations that are sparsely ionizing (radiations of a low LET value). The general finding is that with x-rays the radio-sensitivity of the cells depends on the cell-cycle time of irradiation. This thesis combines high LET radiations with synchronized mammalian cell cultures to evaluate their radiosensitivity at different times in the cell life cycle. The results are of interest to both radiation biology and radiation therapy.

The following sections of the introduction briefly describe some radiation biology measurements related to this research. The introduction is limited to the development of specific questions

of interest in radiation biology and radiation therapy, while several of the cited references provide comprehensive treatises on various aspects of radiation biology.

B. Dose-Response Analyses

The dose-response relationship is one of the most important in radiation biology. The assay of a biological function after irradiation determines the fractional survival for the given dose of radiation. Radiation studies have been made at all levels of biology (molecular, cellular, and organismal) and generally, two types of dose-response, or survival, curves are obtained. More complex survival curves can usually be reduced to a combination of curves of the two general forms. In Figure 1, Curve A represents an exponential survival curve while Curve B is a sigmoidal curve, with a so-called shoulder in the low dose region when plotted on a semi-logarithmic graph. Both kinds of survival curves have been determined for proliferating mammalian cells depending on the type of radiation used (4) and on the radiation dose-rate (31).

Exponential survival curves are most simply interpreted as singular events causing inactivation of the cell. Mathematically,

$$N/N_o = e^{-kD} \qquad \text{(Eq. 1)}$$

where N/N_o is the surviving fraction of the initial number of cells (N_o), D is the radiation dose, and k is a measure of the cellular response. If the radiation is a monoenergetic beam of charged particles directed normal to the culture surface, the dose can be described by the particle fluence (50):

$$D = \alpha FL \qquad \text{(Eq. 2)}$$

where fluence, F, is the number of impinging particles per unit area, L is the value of LET (units of MeV-cm^2/g or keV/micron of unit density material), and α is the proportionality constant. Then,

$$N/N_o = e^{-kD} = e^{-AF} \qquad \text{(Eq. 3)}$$

where A = A(L) is the inactivation cross-section for the radiation characterized by L. This inactivation cross-section is a probability factor for a given radiation. If it were related to

Fig. 1 Survival curves discussed in text: (A) exponential curve; (B) sigmoid; (C) multi-target curve with extrapolation number of 2.0; (D) dose-fractionation survival demonstrating recovery: curve B determined at time T = 0; and curve D determined by irradiating cultures, previously exposed to 5 dose units, at a later time T = t (optimum).

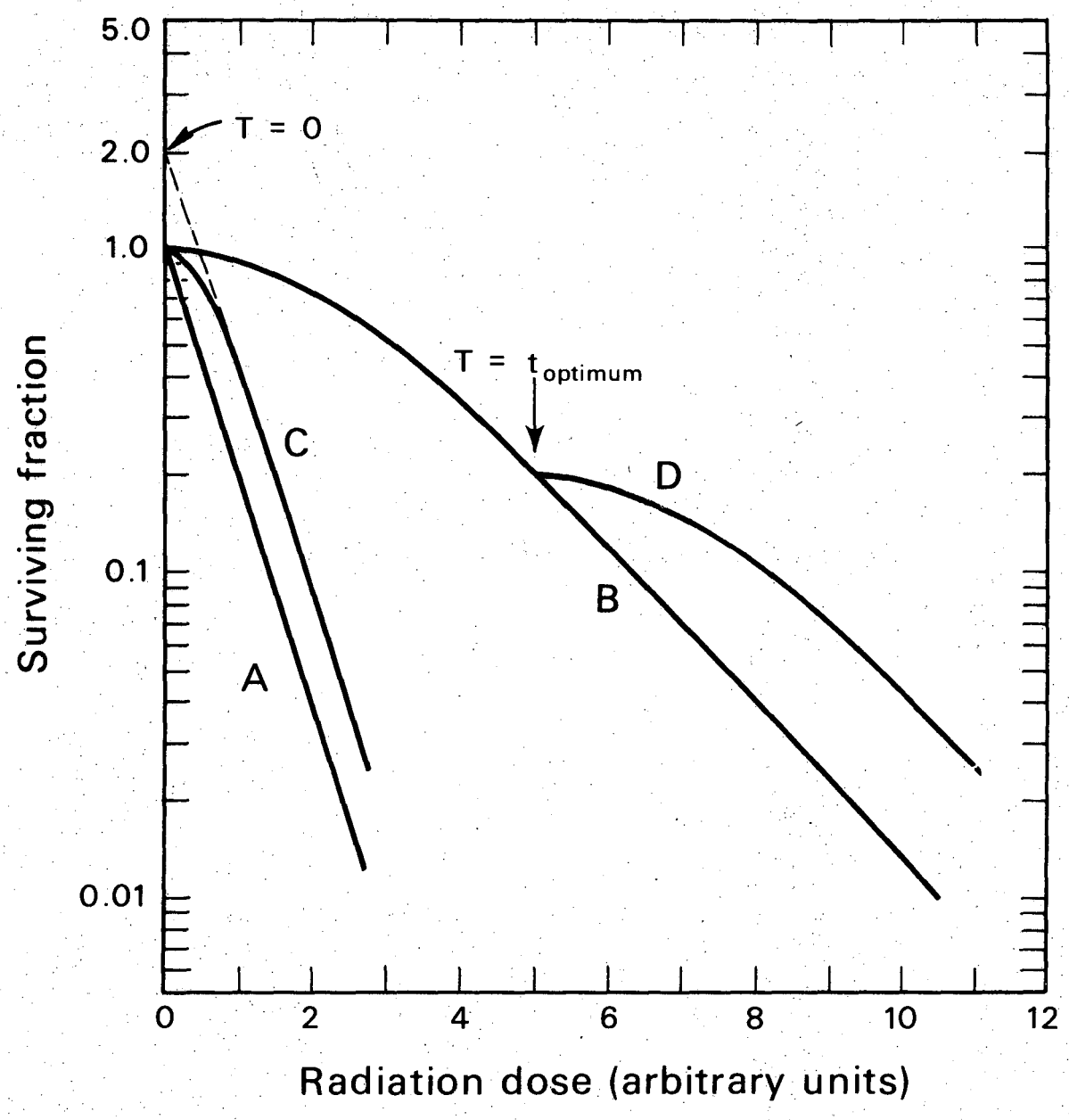
5.0
2.0
1.0
0.1
0.01
T = 0
T = t optimum
A
B
C
D
Surviving fraction
0
2
4
6
8
10
12
Radiation dose (arbitrary units)

DBL 719 5962

an actual biological area, then

$$A = p(L)A_o \qquad \text{(Eq. 4)}$$

where p(L) is the probability that a charged particle crossing the area, A_o, will cause the radiation effect (32).

One inactivating event occurs, on the average, when

$$N/N_o = e^{-1} \cong 0.37.$$

The cellular response constant is often given in terms of this dose, $k = 1/D_{37}$. Thus, the exponential survival curve can be characterized by the D_{37} value or by the corresponding inactivation cross-section,

$$A = \alpha L/D_{37}.$$

When L is determined in units of keV/micron, and the dose is in rads, then

$$A(\text{microns}^2) = 16L(\text{keV/micron})/D_{37}(\text{rads}) \qquad \text{(Eq. 5)}$$

Sigmoidal survival curves have often been interpreted as a requirement of multiple events for an inactivation or as single inactivation events required in multiple sensitive sites (targets), or as some combination of the two (76,17). The multiple "target" concept is applied to some of the experimental results in this report in the following specific way. When two cells are a colony-forming unit and each is separately capable of proliferating to form a colony, then obviously each much be "killed" in order to eliminate the colony. In the simplest of multi-target situations, where the single cell survival curve is exponential, then Curve C in Figure 1, with a so-called extrapolation number of two, results from the multiplicity of two. The slope of the curve at high doses is the same as the single target slope (Curve A in Figure 1). Formally,

$$N/N_o = 1-(1-e^{-kD})^m \qquad \text{(Eq. 6)}$$

where m is the target number. For large doses, Equation 6 can be approximated by

$$N/N_o = e^{-kD} + \ln m \qquad \text{(Eq. 7)}$$

Equation 7 shows explicitly the extrapolation number. If there

exists a mixture of multiplicities in the culture, then m, the extrapolation number, is the mean multiplicity (22).

Most sigmoidal survival curves have high-dose regions that are approximately exponential. The slope of this portion of the curve therefore has a D_{37} value (sometimes referred to as D_o).

Efforts to gain further information about radiation dose-responses have included variation of experimental conditions in an attempt to find interpretable modifications in the response. In studies with cultured, mammalian cells, both chemical and physical modifications have been used, including protective agents, sensitizing agents, and variations in radiation LET. With techniques to obtain synchronized mammalian cell cultures, the physiological state in the cell life cycle is also an inherent radiation "variable". That is to say, as mentioned above, there is a cell-cycle variation in radiation sensitivity, or an "age-response", at least with regard to x-irradiation (56).

The distinction must be made between the cell life cycle as a parameter and other modifying parameters. The study of the age-response can be linked, at least in theory, to specific events in the cell cycle in the attempt to describe radiation sensitive sites and damage mechanisms. With this potential, a great number of experiments originally done with exponentially growing cultures also have been done with synchronized cultures, including the effect of modifying parameters on the dose-response.

C. Some Radiation Survival Results with Mammalian Cells

1. Results with different LET radiations

When radiations of different LET are used to determine survival curves of exponentially growing mammalian cell cultures, the most dramatic feature is a change of curve shape, from a sigmoidal curve with low LET radiation to an exponential curve with a high LET radiation. This feature has been observed with different cell lines and different irradiation techniques (16,7,70,63). Some differences exist in the cited results but in each case there is a consistent trend of increasing cell killing effectiveness per unit dose with increasing LET of the radiation. At the highest

LET values currently available, and beyond that which results in exponential survival curves, the trend is reversed as expected for a wasting of dose along the densely ionized track of the incident particle. With other cell systems, very high LET radiations may be most effective but without a change in survival curve shape from sigmoidal to exponential (40,46,49,42).

The calculated inactivation cross-section from the exponential survival curves is large and has been noted by Barendsen, et.al., (7), to be nearly the observed average cross-section of the cell nucleus. The precise correlation of inactivation cross-section with nucleus cross-section would imply that the passage of a single, high LET particle through the nucleus is sufficient to inactivate a cell. Some other reported cross-section values (see Ref. 44, Table II-9) are slightly smaller than the average nucleus. Evidence implicating the nucleus in whole or in part is reviewed in section I.D. In Table I., a comparison is made between the inactivation cross-section of several mammalian cell lines, irradiated as asynchronous cultures, and the average cross-sectional area of the cell nucleus. In particular, the results obtained for different cells at the same irradiation facility suggest a larger inactivation cross-section for the cells with a larger nucleus: T-1 values greater than M3-1 values, as obtained by Todd at the Berkeley Heavy Ion Linac (HILAC); and HeLa values greater than $CH2B_2$ values as obtained at the Yale HILAC. The inactivation cross sections were obtained for exponential survival curves that did not deviate measurably from being exponential. There exists a possibility of small, experimentally-masked variations, however, which could result from different nuclear sizes in an asynchronous culture. Also, it has been suggested (80) that an exponential curve can be formed from a mixture of sigmoidal curves. Each sigmoidal curve could represent the dose-response of part of a heterogeneous population. By synchronizing cells, one can examine more closely the relationship of the high LET radiation response and the cell life-cycle.

Table 1. Reported Inactivation Cross-Sections for Various Cell Lines

Cell Line and Approx. Nuclear Area	Charged Ion .....(kev/μ)	Inactivation Cross-section (μ^2)	Reference
T-1 (Human Origin) 90-100 μ^2 (modal)	^{12}C.....220	53	Todd (70)
	^{14}N.....300	56	
	^{16}O.....385	66	
	^{20}Ne.....580	90	
	^{20}Ne.....1160	92	
	^{40}A.....1940	148	
M3-1 (Chinese hamster origin) 50 μ^2 (modal)	^{12}C.....220	50	
	^{40}A.....1940	121	
T-1 (Human Origin)	^{4}He.....110	31	Barendsen, et.al. (7)
	^{4}He.....140	35	
	^{4}He.....166	34	
HeLa (Human Origin) 100 μ^2	^{12}C.....190	55	Deering and Rice (16)
	^{16}O.....350	54	
$CH2B_2$ (Chinese hamster origin) 40 μ^2	^{16}O.....351	40	Skarsgard, et.al. (63)
	^{20}Ne.....561	44	
	^{40}A.....1950	62	

2. Radiation Age-Response

All proliferating mammalian cells studied so far show variations in sensitivity to x-rays at different times in the synchronized cell life cycle. The age-response has been reviewed (19,56) with respect to similarities and dissimilarities between cell lines. In Chinese hamster cells (used in the experiments reported here), the age-response is a variation in sensitivity mostly due to variation in size of the survival curve shoulder. However, the age-response of cells of different animal origin do not show the same kind of survival curve variation. There are also temporal differences in the age-response of different cell lines (56) and a difference induced by varying the culture conditions (29).

There are only a few reports of age-response using high LET radiation. Fission neutrons (58), 14 MeV neutrons (30), and accelerated boron ions (refered to in Ref. 19) have been used to irradiate Chinese hamster cells. The age-response is similar in these cases to that of low LET radiation but with a lesser variation in sensitivity. This reduced age-response is suggestive that with higher LET radiation the age-response may become constant as predicted from the exponential survival curves obtained with asynchronous cultures. As noted above, other possibilities are not excluded.

3. Dose-Fractionation Experiments

In their classic experiments on recovery from radiation damage, Elkind and Sutton (21) used the technique of comparing single doses of low LET radiation with the equivalent doses delivered in two parts separated in time. With optimum time of dose separation, the surviving cells after the first dose exhibited a survival curve with a full shoulder indicating a process of recovery from sub-lethal damage (for example, Curve D in Figure 1). Experiments of this type with radiations of different LET have shown this recovery occurs except with very high LET radiations (22,72). Elkind has suggested, in a recent review (19) based on such results and others, that the existence of a shoulder in a survival curve may of itself imply this recovery process. If this is so, the age-

response of Chinese hamster cells, which is primarily due to variations in the survival curve shoulder width, would reflect mostly a variation in the recovery phenomenon.

Dose-fractionation experiments with asynchronous cultures show not only changes due to recovery processes, but possible radiation-induced changes in the distribution of cells in the cell life cycle. That is, the survivors of one dose may progress from a cell phase that is relatively radiation resistant to one that is sensitive. Dose-fractionation experiments with synchronized cultures emphasize this latter variation and can therefore be indicative of an age-response. Skarsgard, et. al. (63) reported dose-fractionation experiments of synchronized cultures of Chinese hamster cells. The results can be interpreted as showing an age-response although any interpretation is rendered difficult by possible radiation-induced sensitization or by inhibition of the cells' progress through the cell cycle.

4. Chemical Modifying Factors

Radiation studies of exponentially growing mammalian cell cultures containing protective or sensitizing agents have been made using radiations of different LET values. In summary, such agents are maximally effective with low LET radiations whereas they have little or no effect on survival after high LET irradiation. These studies have included the effect of protective agents, such as glycerol and cysteamine (6), and oxygen and analogs of DNA* precursor molecules as sensitizing agents (4,5,70,75).

With synchronized cultures, Kruuv and Sinclair (37) and Sinclair (57) have studied the low LET age-response in the presence of oxygen and cysteamine, respectively. Although the oxygen was equally sensitizing at all cell-cycle times, the cysteamine exhibited a differential protective effect. Its protection was minimal at the most radiation sensitive cell-cycle times so that the low LET age-response is partially reduced.

---

*DNA = deoxyribonucleic acid

The fact that chemical modifiers are effective with low LET radiations and not with high LET radiations can be interpreted as a difference either in the kind of molecular structure that is lethaly damaged or in the kind of lesion produced in the same molecule (22). If the kind of molecular structure involved is different, between the low and very high LET radiations, then a difference in the temporal pattern of the age-response might be observed.

D. The Cell Nucleus in Radiation Studies

As mentioned above, evaluation of the radiation inactivation cross-sections results in a value close to that of the average cell nucleus cross-section in exponentially growing cultures. This does not by itself implicate the nucleus. However, decades ago, Zirkle (81) showed that the nucleus of plant cells is the most radiosensitive region. External irradiation of mammalian cells has been done with microbeams of protons (82), and of alpha-particles (43). In each of these experiments, irradiating the nucleus or the cytoplasm only showed the much greater sensitivity of the nucleus.

Another approach to selective irradiation is through the selective incorporation of a radioisotope into a molecule so that its decay can produce localized damage. This approach, called the suicide experiment wherein damage is accumulated when cells are frozen, clearly implicated the locale of DNA molecules as being more sensitive than other molecules used (11). If the DNA molecules are themselves the radiation-sensitive molecules (the working hypothesis of many; for review, see Ref. 44), then the extent to which the DNA is uniformly sensitive and spread throughout the nucleus could be the extent to which the nucleus as a whole is the sensitive site for particulate irradiation.

Electrons of different energy, and ones therefore exhibiting different depths of penetration, have been used to irradiate either interphase cells or metaphase cells (78). With the interphase cells, the results were interpreted as showing a radiation sensitive "shell" at a depth of penetration implicating the outer

regions of the nucleus. In that study, the sensitive nuclear "shell" was compared to the "shell" of DNA synthesis (18). The results suggest that the geometric cross-section of the nucleus could be sensitive to high LET radiation.

The evidence implicating DNA as at least part of a sensitive site for low LET radiation, colony-forming death is substantial (44, 35, 64). Alper (1) has proposed that there is a second sensitive site which she relates to the membrane in bacterial systems, but as an entity in higher cells as well. The membrane is hypothesized as being the site increasingly effected with increasing density of ionization at higher LET values. The external microbeam irradiations indicate that, if this second target exists in mammalian cells, it is not just the plasma membrane, but perhaps the nuclear membrane.

The above review suggests that the nucleus as a whole could be the "target" for high LET radiation. The asynchronous survival curves suggest the inactivation cross-section is single valued, and thus independent of the cell cycle. Yet, the nuclear constitutents are doubling in mass and therefore probably increasing the nuclear dimensions.

E. Restatement of the Problem

The synchronized cell, high LET radiation studies were undertaken to answer the following questions:

(1) What is the high LET age-response?

(2) What does the high LET age-response contribute in the evaluation of applying high LET radiations for therapeutic purposes?

(3) If the high LET age-response is not a constant: (a) what is its temporal relationship to the x-ray age-response (that is, are the same molecular structures implicated for low and high LET radiations); and (b) what is its temporal relationship to nuclear dimensions?

(4) If the high LET age-response is invariant, how does the inactivation cross-section correlate to the nuclear cross-section at all cell-cycle times?

II. MATERIALS AND METHODS

A. General Considerations

Studies concerned with events at different cell-cycle times in a population of proliferating mammalian cells can be done in a variety of ways. In an asynchronous population, time-lapse micrography has been used to determine the cycle time of individual cells with respect to their previous mitosis. At that time, some measurements can be made on the single cells (54). For radiation studies using colony-formation as the endpoint, this approach is not practical. Instead, techniques of synchronizing cultures have been developed.

Synchronizing procedures for cultured mammalian cells have been reviewed elsewhere (for example, Ref. 59). Briefly, in asynchronously growing cultures one can select a subpopulation of cells for study by separation or selective killing of other cells; or some transition point in the cell cycle can be blocked by physical treatment or chemical agent until all the cells have progressed through the cycle to that point; or a combination of the two can be used. Of these various procedures, many mammalian cell biologists have found mitotic selection to be the most attractive means of synchronization due to its simplicity. The use of cell-cycle inhibiting agents generally inhibits a specific cell process and not others, thereby introducing unbalanced growth which may distort radiation sensitivity measurements. The technique of mitotic selection was used in all the experiments on synchronized cultures in this report.

In mitotic selection, cells loosely attached to the growth surface are selectively removed by hydrodynamic shear. This method is based on the observation that during mitosis and for short times before and after mitosis, cells are rounded and more loosely attached than other cells. Mitotic selection of cultured mammalian cells was first accomplished (67) by pipetting culture medium across the growth surface. Since then, mechanical shaking of culture containers has most often been applied in which the culture medium is washed back and forth across the growth surface to dis-

lodge loose cells.

Various procedures have been added to the basic technique in an attempt to enhance the yield and yet to keep a high percentage of mitotic cells in the selected population. Examples are the use of culture medium with a minimum calcium concentration (52), or brief chilling of the culture a few hours before the mitotic shakeoff (60), or repeated shakeoffs at short intervals with discarding of the early cell suspensions (45). However, these procedures, when added to the experimental technique described below, did not result in substantial improvement in both yield and percent mitotic cells.

The fraction of cells in all stages of mitosis is called the mitotic index. Synchrony by mitotic selection can be evaluated by the mitotic index of the initial cell suspension. However, it may not reflect the degree of synchrony at later times following selection. There is an inherent decay of synchrony due to variation from one cell to another in their cell duration (62) as well as the potential loss of synchrony due to subsequent treatment of the cultures. For these reasons, the most appropriate means of evaluating synchrony was to monitor the progress of synchronized cultures from the time of selection to at least the final experimental time.

The cell cycle is commonly defined by the DNA synthesis period and mitosis, both of which can be monitored in pulse-labelled autoradiographs. The pattern of DNA labelling and the number of cells in a culture as a function of time are measures of growth and of synchrony (59,79,23,10). The number of cells can be closely approximated in a series of autoradiographs by observing the average number of cells per microcolony (60). The determination of multiplicity of cells per colony-forming-unit was, in addition, necessary to account for this multi-target factor in the survival curves. The assumption is made that non-viable cells are distributed the same as the multiplicity distribution. Pulse-labelled autoradiographs were used as the basis for evaluating the degree of synchrony and multiplicity in the radiation experiments.

Synchronized cultures have been used to study cell-cycle sensitivity to various environmental effects. When a cyclic variation in sensitivity results, such responses can sometimes be useful, in reverse, to evaluate the degree of synchrony. Both x-rays and hydroxyurea can be so used, theoretically. The x-ray response may be an extremely sensitive means of evaluating synchrony but it is apparently also sensitive to biological variation not yet well understood, including differences between cell lines and between clones (19,4). The toxicity of hydroxyurea is apparently directly related to DNA synthesis only (55) so that within a practical range of concentrations it can be used to measure the degree of synchrony in a culture. Both x-rays and hydroxyurea have been used in these experiments for comparative evaluations.

The major limitation to mitotic selection for cell-cycle studies is the fact that a small fraction of a population is selected. The yield of cells in mitotic selection is related to the fraction of mitotic cells in an exponentially growing culture which is, in turn, inversely proportional to the doubling time of the cultured cells. This was one consideration in determining which of the several, popular radiation biology cell lines was to be used. In addition, a short doubling time was advantageous in the scheduling of experiments using the heavy-ion accelerator. Most important, however, was the choice of a cell line which had been used successfully in mitotic selection experiments.

B. Chinese Hamster Cells *in vitro*

1. *Cell Line*

The cell line used in these experiments was originally derived from female Chinese hamster lung tissue (25). The particular subline, designated V79-S171, was obtained from Dr. Warren K. Sinclair, Argonne National Laboratories, who has cultured it for its mitotic selection characteristics and who, with collaborators, has studied many basic properties of it including cell-cycle radiation effects (58,37,57,61,2).

2. Growth Conditions

The V79 cells were grown in medium EM-15 (55) for stock and experimental purposes. This medium, made in batches in the 500 ml. bottle of commercial saline, consists of:

Puck's Saline F	500 ml (GIBCO)*
TC Vitamins Eagle (100x)	5 ml (DIFCO)+
TC Amino Acids HeLa (100x)	5 ml (DIFCO)
L-Glutamine (200mM)	5 ml (GIBCO)
Penicillin (10,000 units) and Streptomycin (10,000 mcg/ml)	5 ml (GIBCO)
$CaCl_2$-$2H_2O$ (33.3% (w/v))	0.15 ml --
Fetal calf serum	90 ml (GIBCO)
1N NaOH to adjust pH to about 7.4	

Stock cultures and cultures grown to the colony end point were kept in an incubator (National Applicance Company, Portland, Oregon) regulated at 37° C and with a humid atmosphere of air plus 3% CO_2. Culture containers for all situations were polystyrene tissue culture containers (Falcon Plastics, Oxnard, California).

Stock cultures were maintained in exponential growth as judged by the appearance of the culture including the color of the medium since stationary phase cultures are characteristically more acidic according to the phenol red indicator in the medium. A second means of judging exponential growth is by routine electronic counting (Model F Coulter Counter, Coulter Electronics, Inc., Hialeah, Florida) of samples at times of subculturing. The cell counts are useful since the EM-15 medium supports a limited amount of V79 cell proliferation so that exponential growth is limited according to an ultimate cell number per volume of medium (53). Subculturing for maintenance of cells in exponential growth was done by a standard method (22) with 0.03% (w/v) trypsin (Worthington Biochemical Corporation, Freehold, New Jersey) in Puck's Saline A (GIBCO).

---

*GIBCO - Grand Island Biological Company, Berkeley, Calif.
+DIFCO - DIFCO Laboratories, Detroit, Michigan.

A stock of cells was maintained, with 10% (w/v) methyl sulfoxide (DMSO) in the medium, frozen in liquid nitrogen. These cells were frozen within a few subcultures after receipt from Argonne National Laboratories. On three occasions during the course of these experiments, growing stocks were replaced from the frozen stocks.

3. Criterion for Radiation Survival

The criterion of colony-formation for cultured mammalian cells was originally established as a minimum of fifty cells in a colony to define, in effect, unlimited proliferative capacity (47). This criterion has been investigated and although some differences in dose-response curves are observed with different criteria, they generally are slight (21,70,74). The experiments reported here used a colony-forming growth period of six days before staining with a drop of 1% (w/v) methylene blue in distilled water per milliliter of growth medium (22). A ten-power "dissecting" microscope was used to score colonies of sizes corresponding to about fifty cells and more.

C. Synchrony Procedure

1. Mechanical Shaker

A mechanical shaker (see Figure 2) was developed by building a platform on a wrist-action shaker (Burrell Corp., Pittsburgh, Pa). The shaker operates at a frequency of 330 cycles per minute with a variable degree of rotation per cycle. The culture growing surfaces were at a radius of 24.5 cm and the degree of rotation used for mitotic selection was a dial setting between 2 and 3 which corresponds to a motion that is largely horizontal with a displacement of about $\pm$ 2 cm. A greater displacement and thus more vigorous shake is achievable but with a resultant splashing and foaming of the growth medium.

2. Synchrony Protocol

Parent cultures for mitotic selection were grown in 250 ml plastic flasks with a 75 cm^2 growing surface essentially rectangular in shape. Cultures were grown for 30 to 36 hours to achieve

Fig. 2 Mechanical shaker with culture flasks in place on the platform.

Fig. 3 Phase contrast photographs of a colony in a 40-hour culture of V79 cells. (A) Viable cells 15 minutes before fixation. (B) Fixed, hydrated cells stained with toluidine blue.

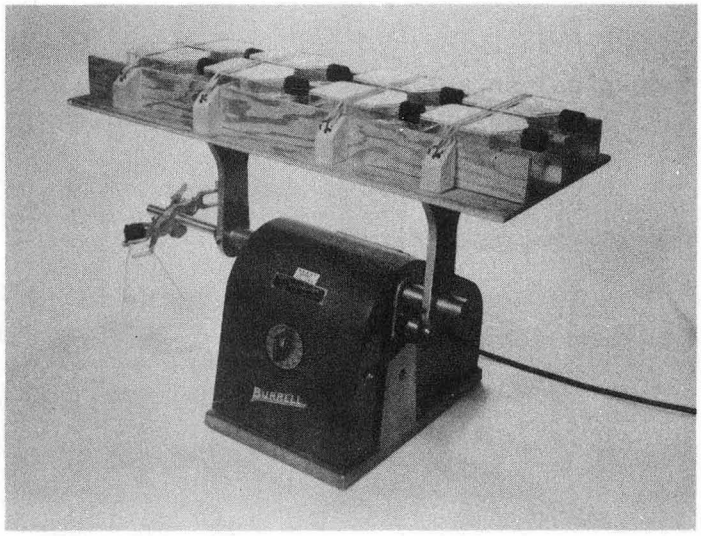

Fig. 2 Mechanical shaker with culture flasks in place on the platform.

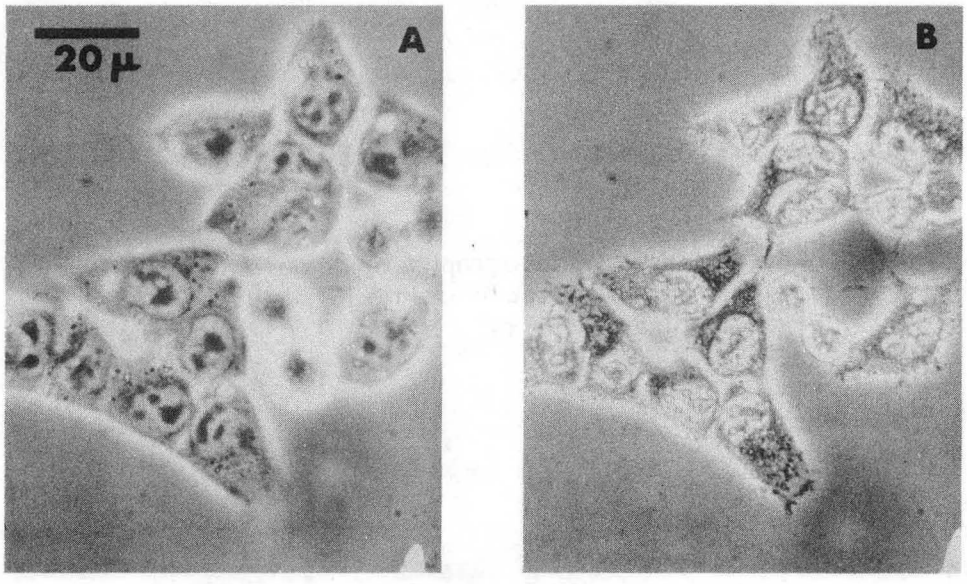

Fig. 3 Phase contrast photographs of a colony in a 40-hour culture of V79 cells. (A) Viable cells 15 minutes before fixation. (B) Fixed, hydrated cells stained with toluidine blue.

XBB 718-3962

small colonies but with adequate time for development of exponential growth. In addition, if a contaminant were accidentally present in a flask, this time would allow its growth to an observable extent.

At the synchronizing time, the growth medium (usually 15 ml with growth to a cell density of about 3 x 10^6 cells per flask) was replaced with 5 ml fresh EM-15 medium prewarmed to about 37° C. The flasks were shaken for one minute and decanted into a sterile glass bottle. Usually, four to eight flasks were handled together. The decanted suspension was vigorously pipetted with a glass pipette to break apart cell clumps and a sample was counted electronically. From the counted cell concentration, generally 5-10 x 10^3 cells/ml, a dilution series was prepared for experimental purposes. For radiation experiments, the dilution series was used to inoculate 35 mm Petri dishes with either one or one-half ml followed shortly thereafter with fresh media to a total volume of 2 ml. Additional cultures were made up from the original suspension for preparing autoradiographs. The entire preparation of experimental cultures for irradiation was carried out in a walk-in, 37° C incubator, with the exception of electronic counting.

In the rest of this report, synchronized cultures are referred to in order to distinguish from cultures where synchrony was not intended. The degree of synchrony achieved in any experiment varied and of course was never ideal.

D. Synchrony Evaluation

1. Autoradiographs

The suspension of cells from mitotic selection was inoculated into coverslip cultures for serial pulse-labelling during the course of experiments. These cultures were in Petri dishes the same size as for irradiation and grown identically to radiation cultures. Pulse labelling was accomplished with 10 to 12 minute exposures to EM-15 medium containing 1 or 2 microcuries thymidine-methyl-^{3}H per milliliter of medium (^{3}H-TdR, New England Nuclear, Boston, Mass.; specific activity of either 6.7 or 15 Ci/mM). The cultures were rinsed twice with EM-15 medium and fixed at least 10 minutes with acetic-ethanol (ratio 1:3). The coverslips were then air-dried

and mounted on microscope slides for preparation of autoradiographs using liquid emulsion (Kodak NTB2, Eastman Kodak Co., Rochester, New York) in a standard technique (28). Exposure periods were one to three weeks and slides were stained with Giemsa in buffer.

Scoring of the stained autoradiographs included the percent labelled cells, percent mitotic cells, and colony multiplicity for at least 200 cells. Scoring of labelled versus non-labelled cells was readily accomplished with these ^{3}H-TdR concentrations and exposures.

2. Other Techniques

Both x-rays and hydroxyurea were used for comparative determinations of synchrony. The x-ray measurements are described below. A concentration of 1mM hydroxyurea (55) in EM-15 medium was applied to cultures for at least two hours at sequential times after mitotic selection. Two rinses with Puck's Saline F and incubation in growth medium for six days was followed by scoring colony survival the same as for radiation survival.

E. Irradiations

1. X-Irradiations

A Norelco MG150 x-ray machine, with 1 mm aluminum added filtration, was operated at 145 kilovolts, 12 milliamperes, and used to expose samples at a target-to-sample shelf distance of approximately 39 cm. The x-ray beam dose-rate was 190$\pm$5 rad per minute, with a half-value layer of approximately 2mm aluminum, as determined by Fricke ferrous sulfate dosimetry (27). Dosimetry was done with the same size polystyrene dishes and volume of dosimeter solution as used with irradiation cultures. Cultures were exposed to x-rays at room temperature (about 23° C).

2. Heavy Ion Irradiations

The Berkeley Heavy Ion Linear Accelerator (HILAC) was used to irradiate V79 cultures with beams of ^{4}He, ^{7}Li, ^{11}B, ^{12}C, ^{20}Ne, and ^{40}A ions. The various beams, although initially accelerated to the same velocity (approximately 10.4 MeV/a.m.u.) were used with varying degrees of absorption between final acceleration and sample position so that their sample velocities were not all the same (see

Table 2). A previous study (70) indicated that the resultant variation in delta-ray LET contribution due to the variation in ion velocity had no measurable effect on the dose-response curves, at least for the LET values tested.

The irradiation apparatus and techniques are reported elsewhere (50,71,73). Since the heavy-ion beams are horizontal and not all sufficiently penetrating, the growth medium was aspirated from the cultures at the irradiation time. The culture dishes were then positioned in a remotely rotated wheel with a 1/2-mil Mylar cover through which the cells were irradiated. The space between the Mylar cover and growth surface was gassed with humidified air.

The heavy-ion beam dosimetry also has been reported in detail previously (40,70,71). A parallel-plate ionization chamber was used to determine the beam dose-rate and delivered doses. At the actual sample position downstream from the chamber, the doses are slightly different due to intervening material (approximately 4 mg/cm^2 Mylar-equivalent thickness). The sample doses were determined from computed range-energy and LET values in water (39) which were verified by comparing computed values in Mylar with range measurements in Myler (40). Table 1 shows the physical parameters of the heavy ion beams and their sample dose-correction factors. Dose rates were generally 300 rads per minute or greater.

Experiments with cultures synchronized by mitotic selection were usually done with two cell populations. The two populations were synchronized at different starting times, usually 3 to 5 hours apart, and irradiated concomitantly. Thus, cells at different cycle times could be irradiated under the same conditions. This also allowed irradiation of two "halves" of the cell cycle with "half" the necessary accelerator beam time.

F. Measurements of Cell Nuclei

1. Phase Contrast Measurements

Coverslip cultures were placed on microscope slide chambers with EM-15 medium for phase contrast photography of viable cells. The chambers were simply made from parts of two glass slides mounted on both ends of a third slide such that a coverslip could be

Table 2. Properties of the Heavy-Ion Beams (Ref. 40)

Heavy ion	Ion chamber plane			Cell sample plane			Dose correction factor
	Range (mg/cm^2)	Energy (MeV/amu)	LET∞ (keV/μ)	Range (mg/cm^2)	Energy (MeV/amu)	LET∞ (keV/μ)	
^{4}He	130.26	10.12	18.8	125.96	9.93	19.1	1.015
^{7}Li	101.7	10.09	42.3	97.4	9.85	43.4	1.026
^{11}B	54.33	9.63	123.3	50.03	9.17	129.5	1.05
^{12}C	40.75	9.55	179	36.45	8.93	191	1.07
^{20}Ne	18.29	7.34	576	13.99	6.15	656	1.14
^{40}A	12.87	6.88	1690	8.57	5.09	2000	1.19

suspended between the two and the space between the coverslip and third slide could be filled with fluid. The chamber could be photographed and reincubated repeatedly.

Several fields were photographed both early and late in the cell cycle to observe any changes in the cross-section of nuclei. The photographic arrangement used a Zeiss phase contrast microscope and Polaroid film with total magnification of 840X. Picture images were projected onto a sheet of vellum transparency for tracing the outlines of the nuclei, then cutting and weighing to determine their area.

The greatest difficulty in such measurements is due to the three-dimensional shape of nuclei which are not a geometric shape, especially in the early stages of the cell cycle. The maximum extent of the nucleus in its projection onto a plane normal to the microscope light (or radiation beam) is not everywhere in the same focal plane for photography. The maximum cross-section observable when varying the microscope focal plane was therefore photographed.

2. Fixed and Stained Cells

Coverslip cultures from mitotic selection were fixed at different times in order to obtain an estimated average area for the cell nuclear cross-section at these times. Bouin's fluid was gently added to cultures with Puck's Saline F after rinsing away growth medium. The culture dishes were decanted and Bouin's fluid added for at least 30 minutes. The fixed cultures were then rinsed thoroughly with distilled water and stained briefly with toluidine blue (0.1% (w/v) in distilled water). The stain was replaced with distilled water. The hydrated, fixed cells were photographed under 1040X magnification. Photographs were projected onto vellum transparencies for determination of nuclear areas as was done with phase contrast photos.

III. RESULTS

A. Synchronized Cultures

1. The Synchronized V79 Cell Cycle

Synchronized V79-S171 cells, resulting from the synchronizing procedure used in these experiments, produced the typical growth patterns in Figure 4 (open circles). The percentage of cells labeled (Panel A) and the mean multiplicity of cells per colony-forming unit (Panel B) are plotted against the time defined by the shake-off time, T = 0. The phases of the cell cycle are schematically indicated. In this experiment, the phases are less defined in the second cycle than the first, indicating a loss of synchrony with time.

The degree of synchrony for the experiment in Figure 4 and other experiments was evaluated as the labeling index. This index, as shown by Sinclair (59), is in good agreement with other more complex methods of evaluation. It relates the maximum labeling to the minimum labeling that follows in time. The index is the difference between the two labeling percentages. Ideally, the maximum labeling would be 100% labeled cells (all S cells) followed by 0% labeled cells (all G2 cells). The ideal labeling index is therefore 100%. The asynchronous cultures would have an index of 0% since there would be a constant percentage labeled cells in time. In the experiment shown in Figure 4, the labeling index was approximately 67% for the first cycle.

Synchronized cell cycles were found to vary in duration primarily due to a varied G1 phase. This was in part attributable to variations in experimental conditions, particularly in the preparation time of cultures for irradiation experiments. In exponentially growing cultures, the population doubling time was consistently 9.7 to 9.9 hours similar to values obtained by Sinclair and colleagues (2, 62) with this subline of cells. The autoradiographic determination of labeled cells and multiplicity, in cultures established by trypsinization at time T = 0 from exponentially growing cultures, is shown in Figure 4, Panels A and B (closed circles).

Fig. 4 Growth of Chinese hamster cells sampled successively by autoradiography. Open circles for synchronized cells; closed circles for cells trypsinized at T = 0 from an exponentially growing culture. Panel A: Pulse labeling with tritiated thymidine. Panel B: Multiplicity, or average number of cells per colony-forming unit. The cell-cycle phases are schematically designated.

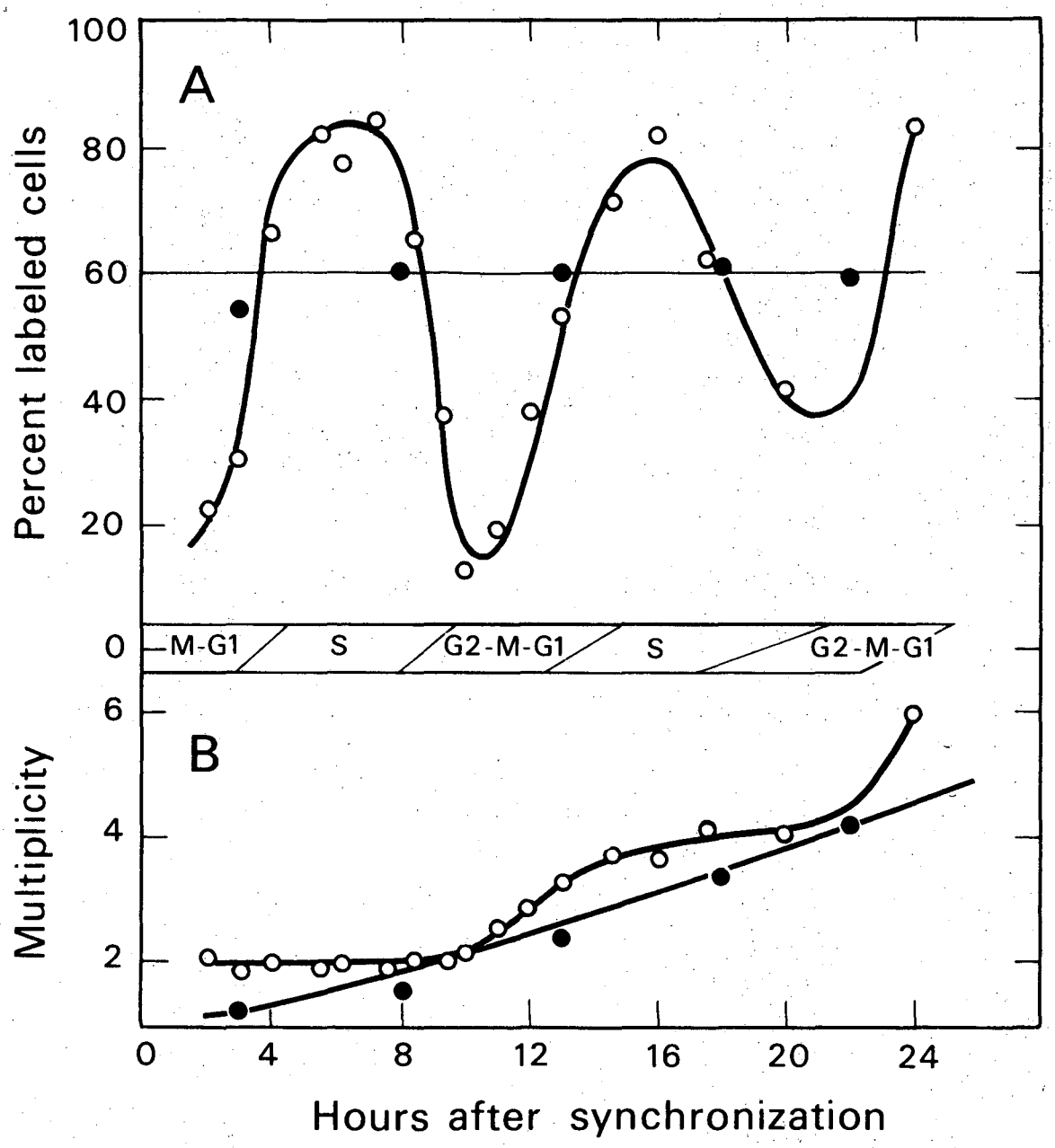
A
B
Percent labeled cells
Multiplicity
100
80
60
40
20
0
M-G1
S
G2-M-G1
S
G2-M-G1
6
4
2
0
4
8
12
16
20
24
Hours after synchronization

DBL 719 5957

Hydroxyurea has been shown to be toxic to mammalian cells during synthesis of DNA (55). In Figure 5, this toxicity to DNA synthesis produces a variation in the synchronized cell, colony-forming survival that mimics in reverse the labeled-cell pattern determined in autoradiographs. The fact that hydroxyurea can kill late S cells in a mixture of S cells and G2 cells was used in one high LET radiation experiment to obtain a survival curve for G2 cells.

2. Cross-Sectional Areas of Cell Nuclei

Figure 3 shows comparative pictures of a colony of cells in a 40-hour culture taken about 15 minutes before and one day after fixation, staining, and rehydration. These and other comparative pictures taken by phase contrast photography indicate that the fixing procedure introduces no or little distortion in the dimensions of the nucleus, for at least a few days when maintained in a water environment.

Bright field photographs were made of synchronized cells fixed at the cell-cycle times indicated in Figure 6. The cells were part of the experiment whose synchrony is shown in Figure 5. The mean cross-sectional area of fifty nuclei is indicated in Figure 6 for times T = 2 and 6.5 hours. For times 3 and 10 hours, the mean area of 110 nuclei is given. The distribution of areas was determined for times 3 and 10 hours as depicted in the right side of the figure. Clearly, an increase in the mean cross-sectional area of cell nuclei is indicated. An increase was similarly determined in serial, phase contrast photographs of several cells as they progressed through their cycle following synchronization.

3. X-Irradiation Sensitivity

Survival curves for V79 cells x-irradiated at different times after synchronization are shown in Figure 7. Survival clearly is varied according to the time of irradiation in the cell cycle. To show this variation directly, the age-response of V79 cells as determined in different experiments, is given in Figure 8. Differences in the measured x-ray age-response may be due to variation in

Fig. 5 Comparison, for synchronized cells, of pulse-labeled autoradiographs and of colony survival for exposure (at least two hours) to 1 mM hydroxyurea in growth medium applied at the various cell-cycle times indicated (error bars denote one standard deviation). In this experiment cultures were delayed at room temperature about 30 minutes following synchronization before incubation.

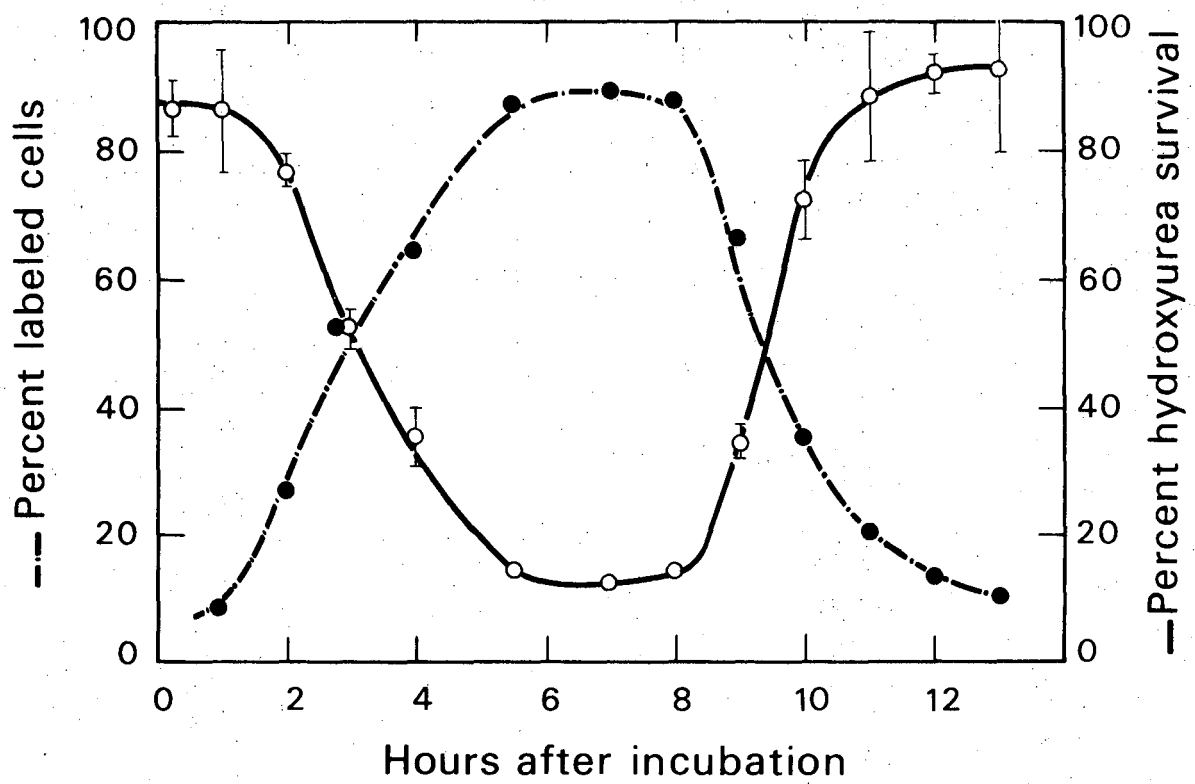
100
80
60
40
20
0
0
2
4
6
8
10
12
Hours after incubation
Percent labeled cells
Percent hydroxyurea survival

DBL 719 5961

Fig. 6 The average cross-sectional area of cell nuclei as a function of time in the synchronized cell cycle (same experiment as in Figure 5). The distributions of cell nuclear cross-sections shown in the right portion of the figure for the 3-hour and 10-hour times were each determined for 110 nuclei.

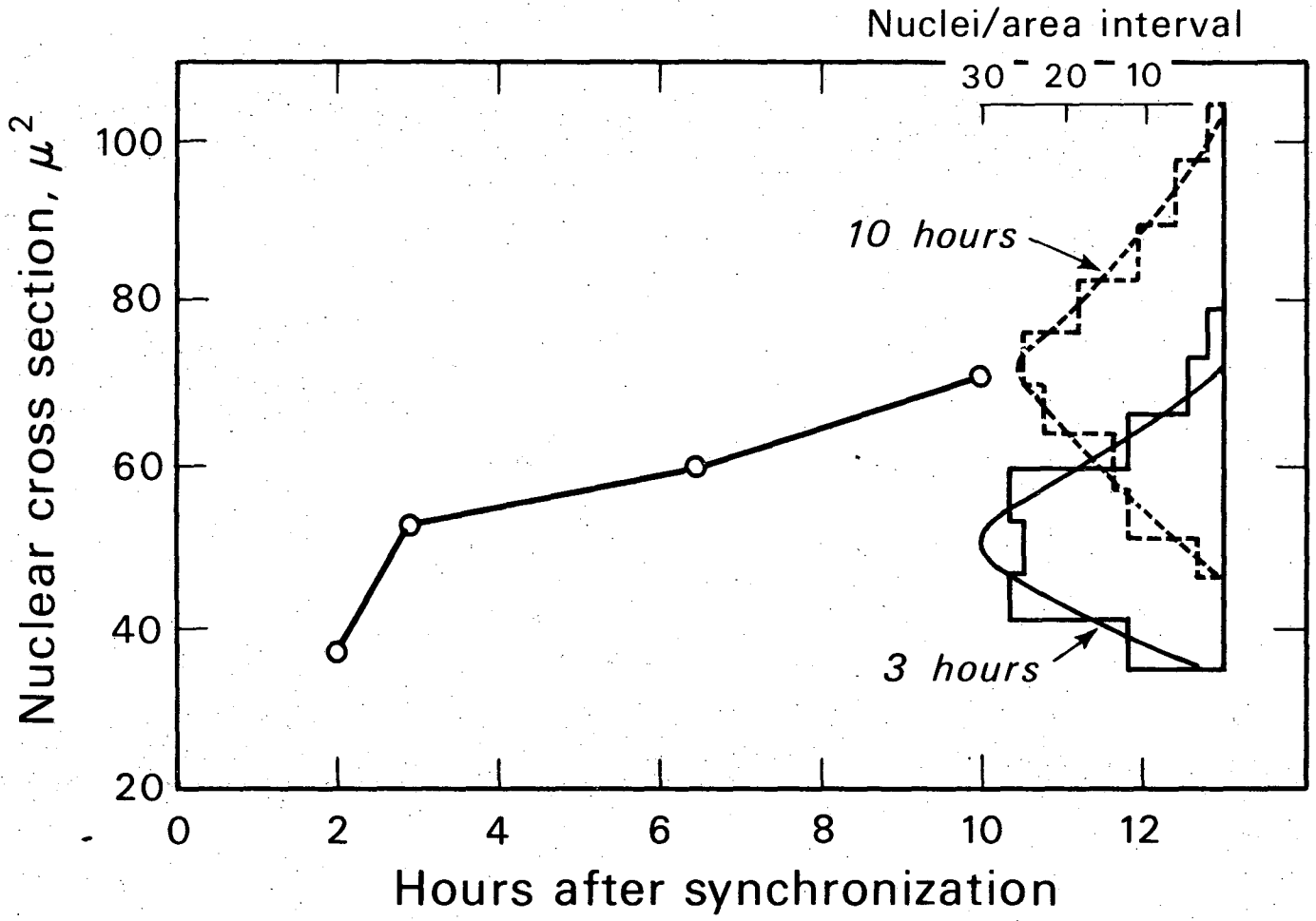
Nuclei/area interval
30 20 10
10 hours
3 hours
Nuclear cross section, μ^2
100
80
60
40
20
0
2
4
6
8
10
12
Hours after synchronization

DBL 725 5312

Fig. 7 Comparison of x-ray survival curves at different times after synchronization (survival curves were not all obtained in one experiment).

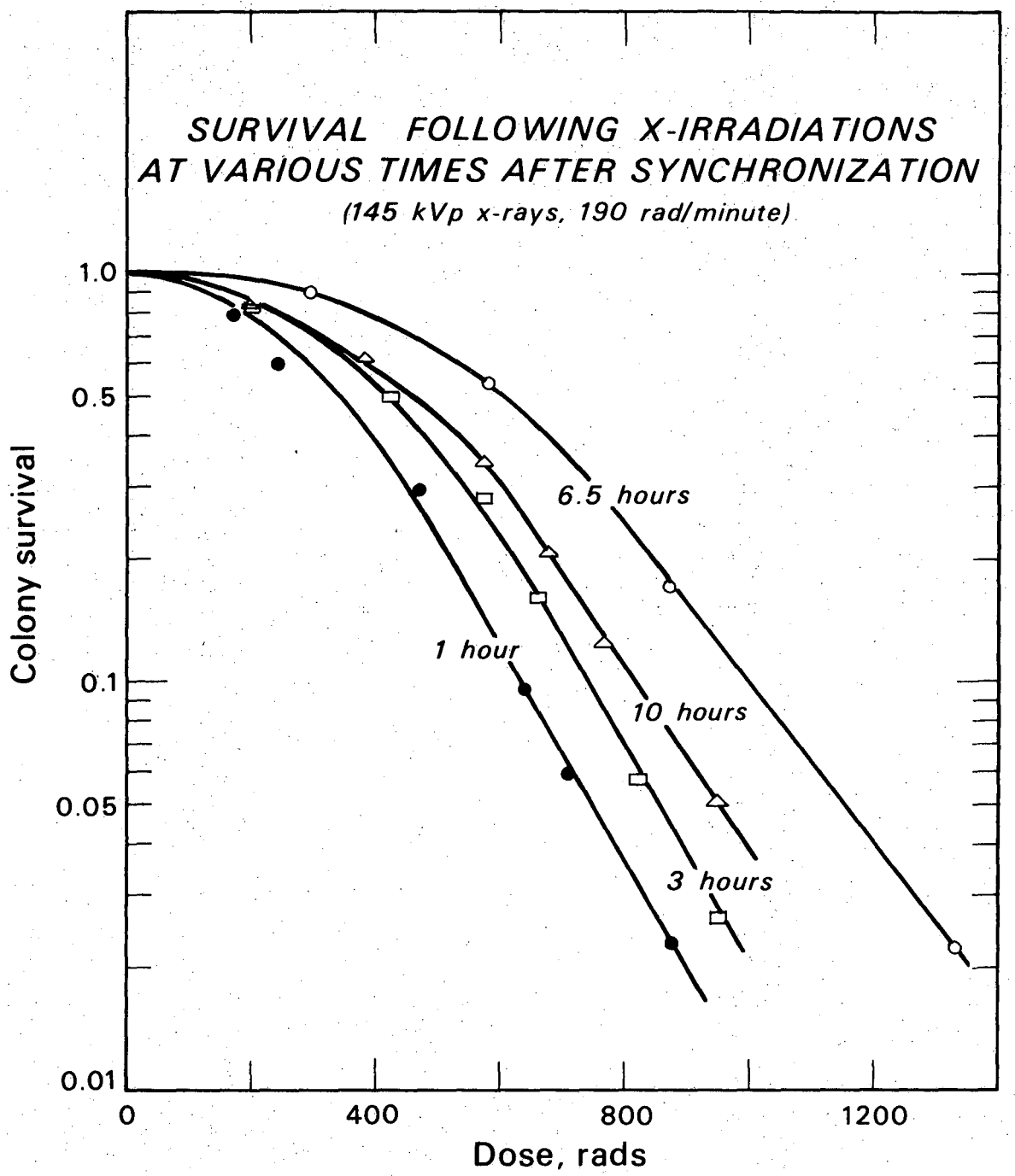

Fig. 8 Panel A: Age-response curves for 950 rads of 145 kVp x-rays. Panel B: Labeling patterns determined by autoradiography. The triangles and curves marked as (1) are from the experiment shown in Figure 4. The circles and curves marked as (2) are derived from separate experiments. The age-response curve (2) was determined from separate experimental curves as in Figure 7; the labeling pattern curve (2) was drawn through the mean values obtained by averaging the labeling pattern data for three heavy ion experiments (error bars denote standard errors). Open and closed squares are data from two successively synchronized populations in one x-ray experiment. Curves marked as (3) are drawn through the open and closed squares.

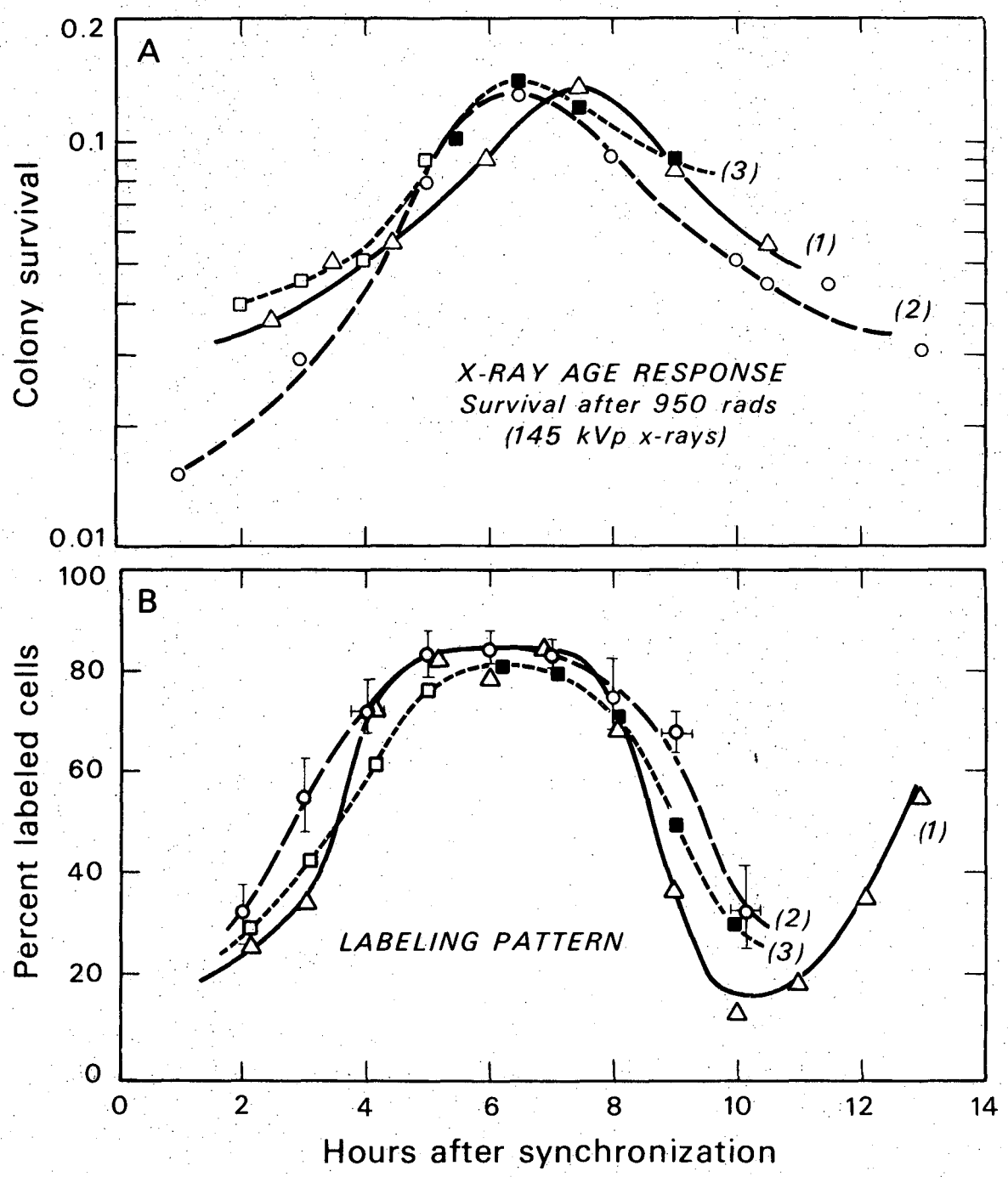
A
0.2
0.1
0.01
Colony survival
X-RAY AGE RESPONSE
Survival after 950 rads
(145 kVp x-rays)
(1)
(2)
(3)
B
100
80
60
40
20
0
Percent labeled cells
LABELING PATTERN
(1)
(2)
(3)
0
2
4
6
8
10
12
14
Hours after synchronization

DBL 719 5965

degree of synchrony alone or due to some biological variation as well. The survival curves and x-ray age-response curves are not unlike those obtained by Sinclair and Morton (61).

B. High LET Irradiations

1. Survival Curves for Cultures Not Synchronized

Irradiations using ^{4}He, ^{7}Li, ^{11}B, ^{12}C, ^{20}Ne, and ^{40}A ions accelerated at the Berkeley HILAC were made to determine the survival curves for V79 cells without synchronization. Figure 9 compares these survival curves. Cultures with multiplicities greater than unity were irradiated to establish the curves similar to that expected for synchronized cultures and the curves are displayed without correction for the multiplicity. The pattern of changing curve shape with varied LET is similar to that obtained by others for mammalian cells as discussed in Chapter I. This changing survival curve shape is readily evident when the multiplicity factor is accounted for in which case Panel B results in curves that are exponential while Panel A curves retain a sigmoidal shape. The survival curve obtained for boron ion irradiation has an uncorrected extrapolation number greater than three as indicated by the dashed line in Figure 9. It is interesting to note that although the survival curve for boron ion irradiation indicates a sigmoidal survival curve for single cells, the slope of the curve in the high dose region is steeper than that for the carbon ion irradiation.

Table 3 lists the asynchronous survival curve parameters determined for each ion, assuming the multiple "target" curve shape, Equation 6. The multiplicities for each experiment are also listed. The parameters were obtained by the general method of handling nonlinear equations of condition for least-squares evaluation (48). This method used a Taylor's expansion about estimated values of the coefficients. The initial coefficient values were obtained graphically and the least-squares calculations were iterated until changes in the coefficient values were smaller than that incurred in rounding off to three digits for tabulation.

Fig. 9 Survival curves for Chinese hamster cells not synchronized. The accelerated ion that was used, and the cell multiplicity in each irradiation were: (A) ^{4}He (1.6), ^{7}Li (1.8), ^{11}B (1.7) and (B) ^{12}C (1.7), ^{20}Ne (1.7), ^{40}A (1.7).

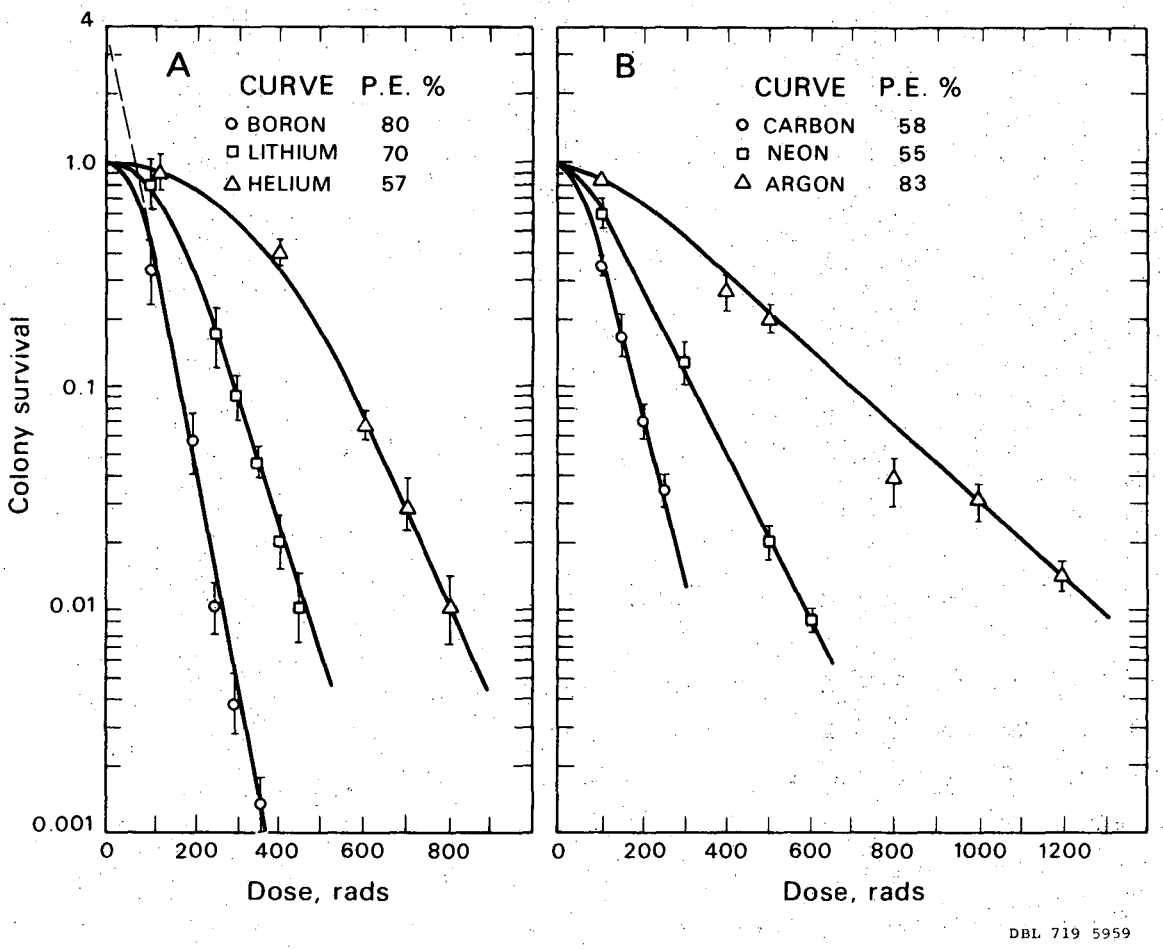
A
CURVE P.E. %
BORON 80
LITHIUM 70
HELIUM 57
B
CURVE P.E. %
CARBON 58
NEON 55
ARGON 83
Colony survival
4
1.0
0.1
0.01
0.001
0
200
400
600
800
1000
1200
Dose, rads
Dose, rads
DBL 719 5959

Table 3. Survival Curve Parameters for Asynchronous Cultures

Ion	Colony multiplicity	Parameters (Eqn.6) m	kx 10^3
^{4}He	1.6	24.2 ± 2	9.4 ± 0.1
^{7}Li	1.8	6.49± .98	14.9 ± 0.4
^{10}B	1.7	3.42± .29	21.1 ± 0.3
^{12}C	1.7	1.88± .14	16.0 ± 0.4
^{20}Ne	1.7	1.70± .12	8.73 ± 0.13
^{40}A	1.7	1.45± .08	3.88 ± 0.08

2. Survival Curves for Synchronized Cultures

Figures 10, 11, and 12 show the survival curves for irradiation of synchronized cultures using accelerated ^{12}C, ^{20}Ne, and ^{40}A ions, respectively. Figures 10 and 11 each show survival curves of single experiments with the corresponding labeling patterns. In each figure, the labeling patterns are compared to the "typical" pattern of Figure 4 which is a more detailed pattern. Figure 12 shows survival data of three experiments with the data grouped according to the approximate cell-cycle phase at the time of irradiation.

The cultures used in the carbon ion irradiation (Figure 10) were derived from the same populations of cells used for the x-ray experiment denoted by open and closed squares in Figure 8, Panels A and B. The divergent treatment for irradiation in separate facilities resulted in only a slight difference in labeling patterns. A substantial x-ray age-response was determined for these cultures. In Figure 10, the solid lines drawn for each curve are the same. The colony multiplicities determined from autoradiographs were

found to have an average value of 1.7 with a variation of less than 0.1 from that average for all the sample times. The survival curve parameters of Equation 6 have been calculated for these survival curves in the same manner as described above and tabulated in Table 4.

The survival curves in Figure 11 (Panel A) were determined for neon ion irradiation. The synchronized cultures produced labeling patterns (solid curves in Panel B) similar to that of the comparison labeling pattern (dashed curve). However, the multiplicities determined for the synchronized populations in the neon ion experiment were different. The open circle data corresponded to a multiplicity of 1.8 throughout the experimental period; the closed circle data corresponded to a multiplicity of 2.0 until the cell-cycle time of 10 hours after which the multiplicity increased. The approximate multiplicity at the irradiation time of 11.5 hours was 2.6. The survival curve lines were drawn to reflect the multiplicity in the extrapolation number. The calculated survival curve parameter values are listed in Table 4.

In Figure 12, the grouped, survival curve data fall along the survival curve line which is drawn the same in all three cases. As for the two previous figures, the argon irradiation survival curve parameters have been calculated and listed in Table 4.

Examination of the data in Tables 3 and 4 indicates that the parameter k changes less than 5% from a mean value for different cell-cycle times and with no discernable pattern. The k values for synchronous survival and asynchronous survival differ by about 5%, 13%, and 0% for argon, neon, and carbon ion irradiation, respectively. The extrapolation numbers in Table 4 are more variable than the culture multiplicities. In general, this variation is within about 20% of the multiplicities, the exception being the neon, 8.5 hour, data. This exception is also unusual in the value of k. Examination of the data in this exception shows a continued downward curvature with dose rather than an exponential curve at high doses. The survival curve parameters would be exaggerated, therefore, and in the direction observed.

Fig. 10 Panel A: Survival curves for Chinese hamster cells irradiated with ^{12}C ions at different times after synchronization. Two synchronized populations are separately indicated by open and closed circles. Panel B: The corresponding labeling patterns for the two populations are indicated with corresponding open and closed circles and with the dashed line drawn through the data. The solid line was taken from Fig. 4, Panel A.

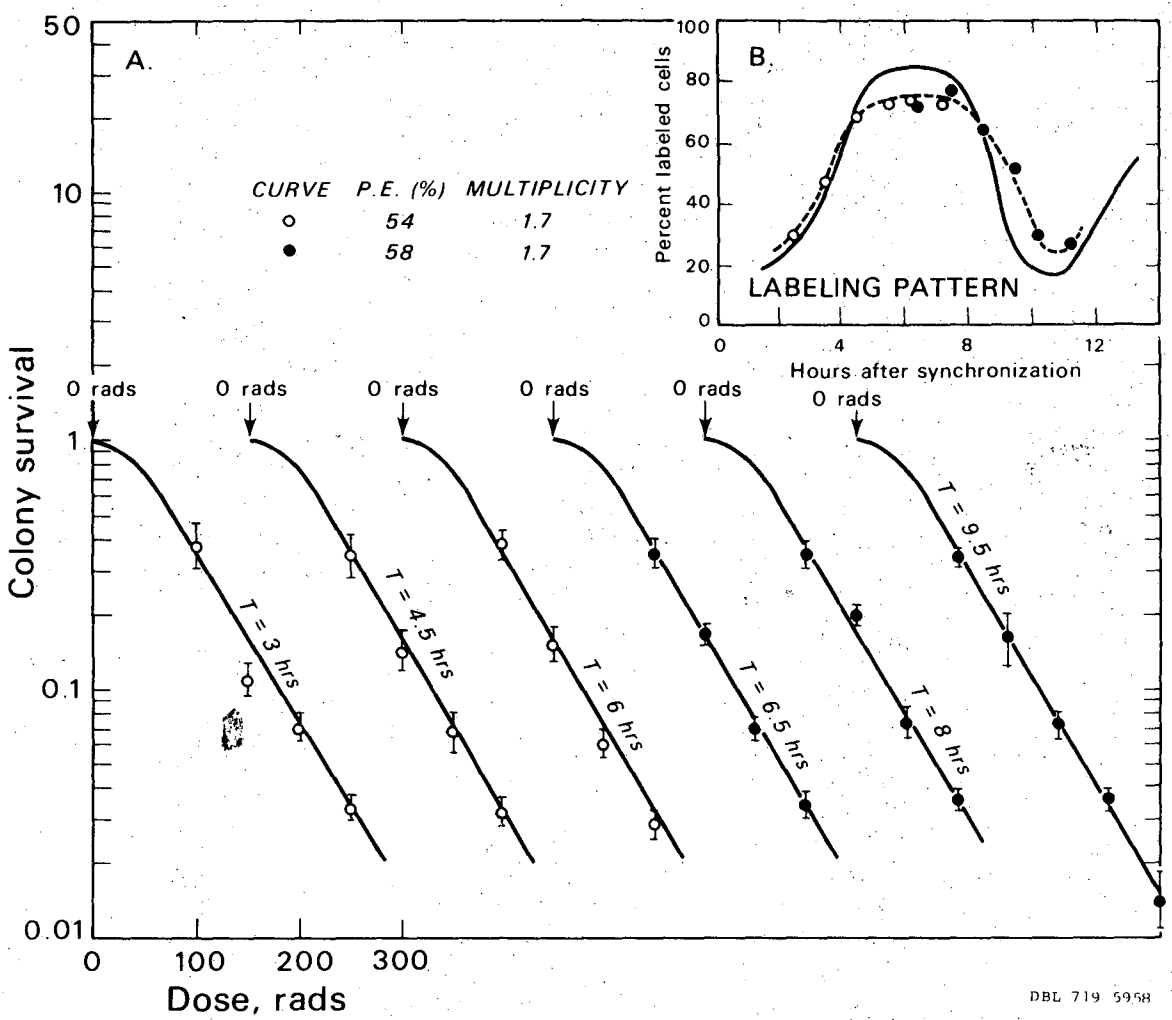
A.
B.
CURVE P.E. (%) MULTIPLICITY
54 1.7
58 1.7
Percent labeled cells
LABELING PATTERN
Hours after synchronization
Colony survival
0 rads
T = 3 hrs
T = 4.5 hrs
T = 6 hrs
T = 6.5 hrs
T = 8 hrs
T = 9.5 hrs
Dose, rads
DBL 719 5958

Fig. 11 Panel A: Survival curves for cells irradiated with ^{20}Ne ions at different times after synchronization. Panel B: The corresponding labeling patterns for the two synchronized populations are indicated with corresponding open and closed circles and with the dashed line drawn through the data. The solid line was taken from Fig. 4, Panel A.

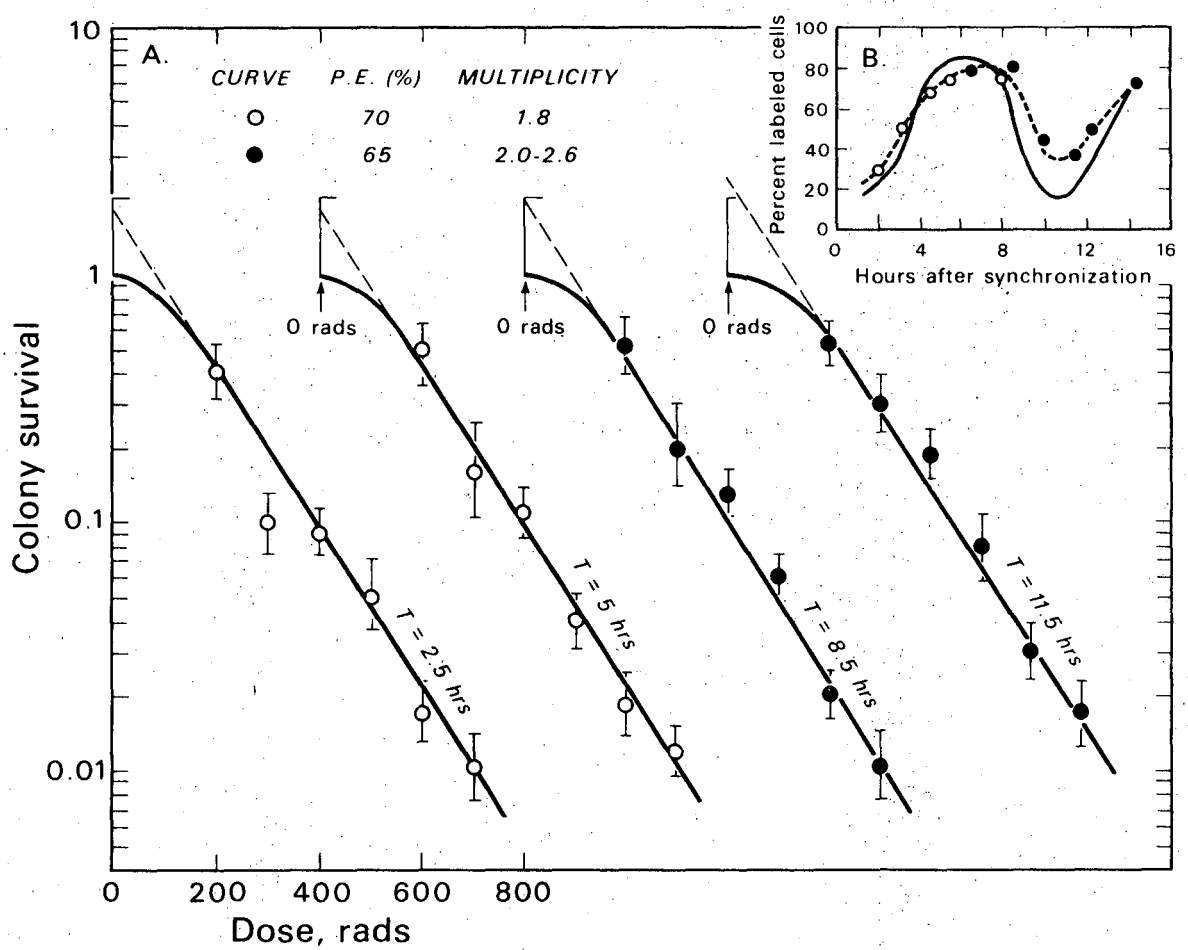
A.
CURVE
P.E. (%)
MULTIPLICITY
70
1.8
65
2.0-2.6
0 rads
0 rads
0 rads
T = 2.5 hrs
T = 5 hrs
T = 8.5 hrs
T = 11.5 hrs
Colony survival
10
1
0.1
0.01
0
200
400
600
800
Dose, rads
B.
Percent labeled cells
100
80
60
40
20
0
0
4
8
12
16
Hours after synchronization

DBL 719 5960

Fig. 12 (A) Survival curves for three experiments of ^{40}A-ion irradiation at different times after synchronization. Curves for separate experiments are grouped according to cell cycle phases for convenience. Experiment one consisted of times 2.5 hours and 9 hours (open circles); experiment two consisted of two populations: (a) 3 hours, 5 hours, 6 hours, and (b) 7.5 hours, 9 hours (closed circles) and 10.5 hours; experiment three was an irradiation at 2 hours. The experimental data all had standard deviations of 12% or less. The labelling index varied from 55 to 70%; plating efficiency varied from 46 to 83%; and the multiplicity in each case was between 1.7 and 1.8.

ARGON ION IRRADIATIONS

LET: 2000 KEV/μ

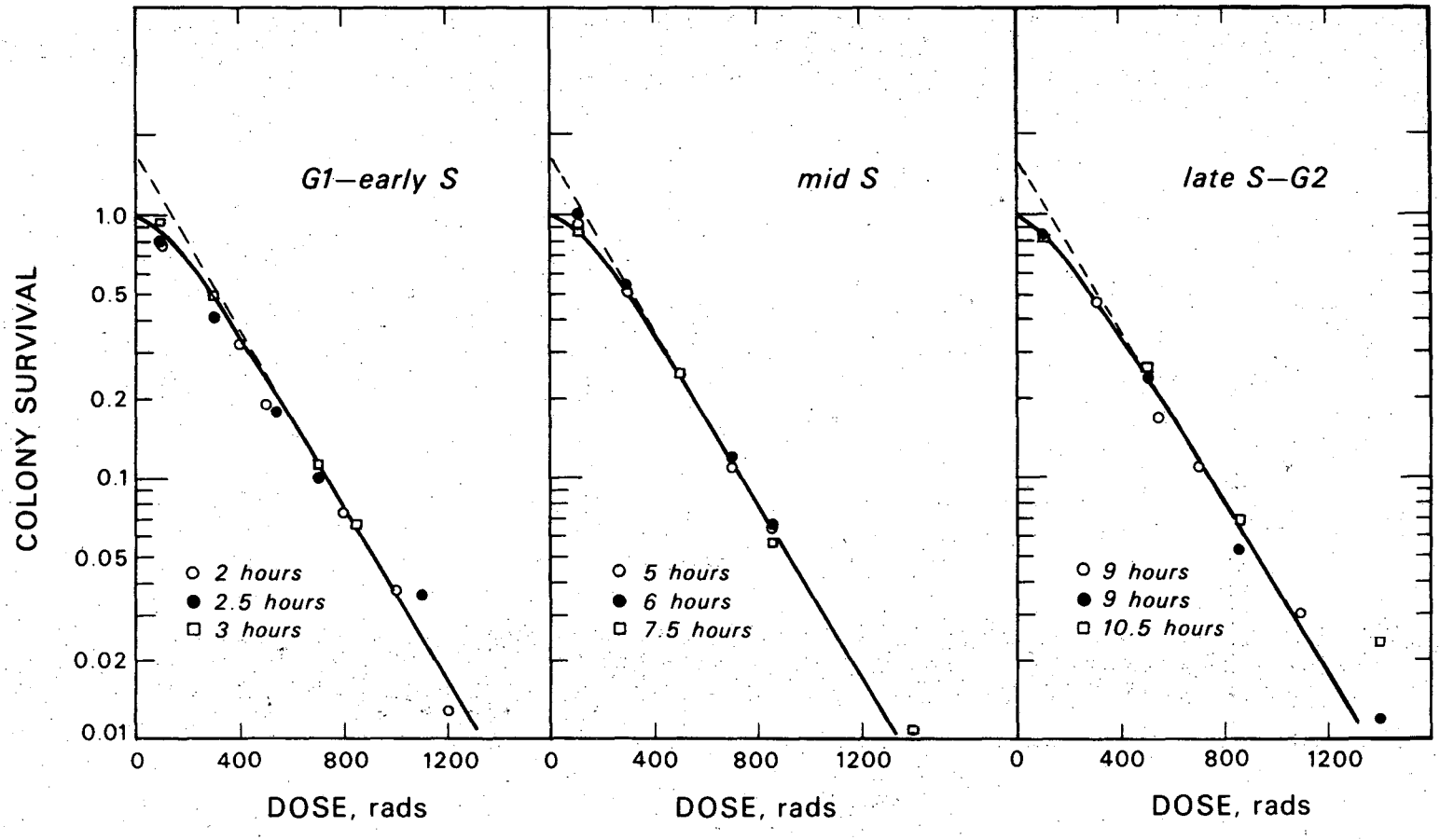

DBL 713-5688

Table 4. Survival Curve Parameters for Synchronized Cultures

Cell time (hours)	Cell multiplicity	Parameters (Eq. 6) m	$k \times 10^3$
	Carbon ions (Fig. 10)		
3	1.7	1.73 ± .15	16.1 ± 0.4
4.5	1.7	1.68 ± .15	15.9 ± 0.4
6	1.7	2.05 ± .13	17.0 ± 0.3
6.5	1.7	1.87 ± .10	16.0 ± 0.3
8	1.7	2.20 ± .13	16.3 ± 0.3
9.5	1.7	1.78 ± .09	15.9 ± 0.3
	Neon ions (Fig. 11)		
2.5	1.8	2.09 ± .42	7.85 ± 0.40
5	1.8	2.00 ± .25	7.53 ± 0.24
8.5	2.0	3.45 ± .38	8.24 ± 0.20
11.5	2.6	3.20 ± .37	7.55 ± 0.24
	Argon ions (Fig. 12)		
G_1 - S	1.7-1.8	1.52 ± .05	3.70 ± .04
S	1.7-1.8	1.70 ± .06	3.75 ± .04
S - G_2	1.7-1.8	1.35 ± .05	3.46 ± .05

Figure 13 shows survival curves obtained in one experiment for separate populations of cells. Curve G2 was obtained by irradiating synchronized cells 9.5 hours after the synchronizing procedure, then treating the cultures with hydroxyurea to assure survival of only G2 cells. This treatment reduced the number of colonies in unirradiated controls by 21%. From autoradiographs, the percentage of colony-forming units consisting of only labeled cells was about 25%. The curve G1 was obtained for cultures 1.5 to 2.0 hours following synchronization. About half of that time the cultures were at ambient temperature. A sample culture pulse-labeled for autoradiography at the irradiation time showed only 13% labeled nuclei. An autoradiograph of the asynchronous cultures showed 60% labeled nuclei. The data for the two populations, G1 and asynchronous, fall along the drawn curve (solid line) reasonably, and the extrapolation number corresponds reasonably with the population multiplicities. The G2 data have been connected by the light dashed curve. The curve might be interpreted as biphasic, for example, indicating two populations with differing extrapolation values. However, such an interpretation would require a population of perhaps 10% of the cells with an extrapolation number of the order of ten. The cultures sampled autoradiographically did not contain any clumps of cells of such multiplicity, implying a significant survival curve shoulder under such an interpretation. It is more likely that the technical necessity of several changes in the culture media, as a consequence of using the cytotoxic drug, contributed to a loss of cells from the cultures. Such a loss is conceivably dose-dependent due to radiation induced mitotic inhibition.

A comparison of the effectiveness of the ^{12}C, ^{20}Ne, and ^{40}A ions in killing Chinese hamster cells is given in Table 5. Since the apparent survival curve extrapolation number is approximately accounted for by the culture multiplicity, the determination of the survival curve slope determines the slope of the single cell survival curve and therefore the inactivation cross-section. The

Fig. 13 Survival curves for cells irradiated with accelerated ^{40}A-ions. Three separate populations of cells were irradiated in one experiment: G2 cells "isolated" by hydroxyurea treatment after irradiation; G1 cells 1.5 to 2 hours after synchronization; and cells trypsinized from exponentially growing cultures. Multiplicities determined for the three cultures were 2.0 (G2), 1.7 (asynch.), and 1.8 (G1). The light dashed curve through the G2 data is discussed in the text.

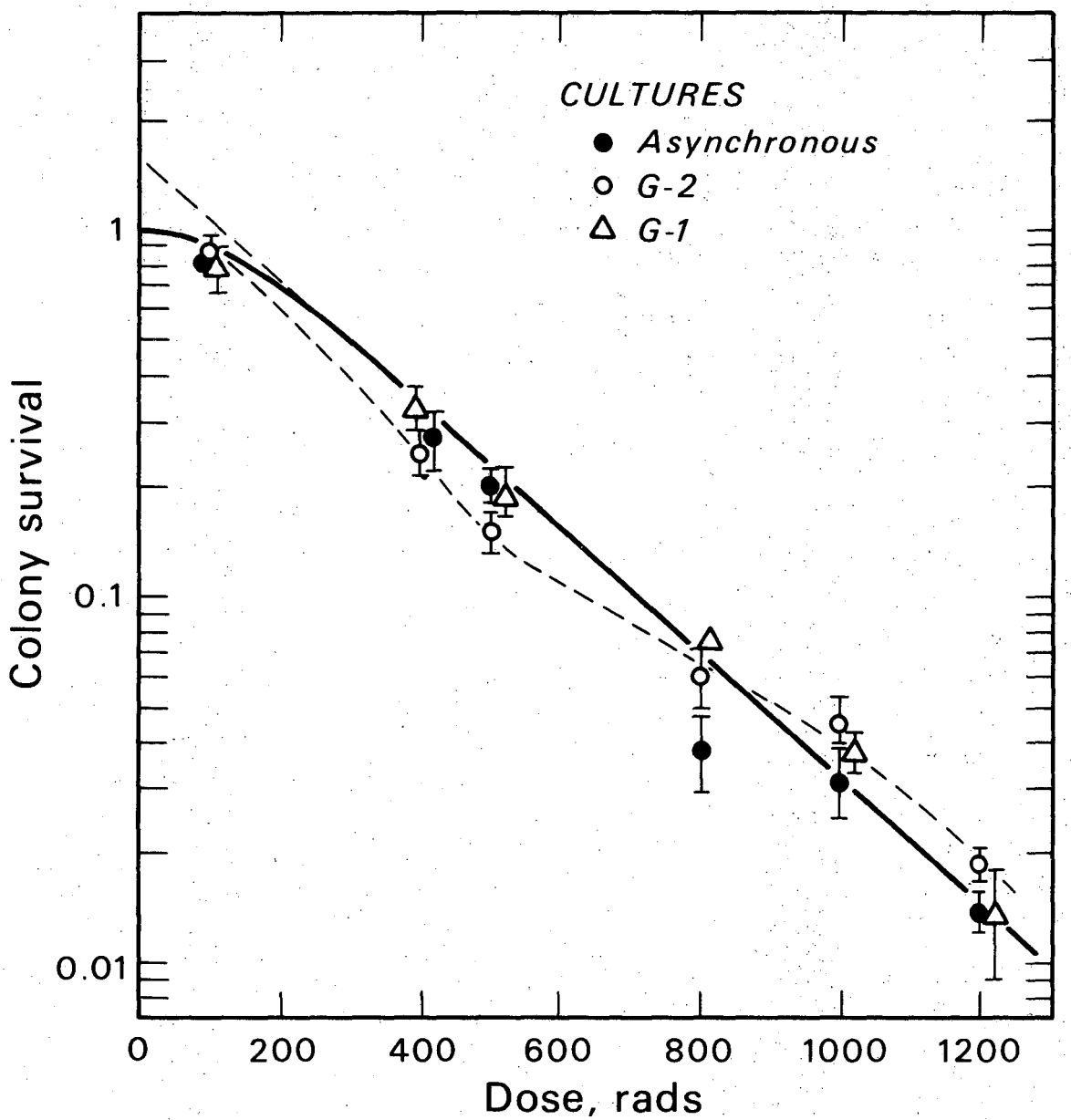
CULTURES
Asynchronous
G-2
G-1
Colony survival
1
0.1
0.01
0
200
400
600
800
1000
1200
Dose, rads

DBL 725 5313

uncertainty in the inactivation cross-section may be of the order of the difference noted between the asynchronous and synchronous survival curve slopes which is greatest for neon ion irradiation (Tables 3 and 4), about 13%.

Table 5. High LET Inactivation Cross-Sections for V79 Cells

Ion	D_{37}** (rads)	Dose correction factor*	D_{37} Corrected	A (micron^2)
^{12}C	62	1.07	66	47
^{20}Ne	129	1.14	147	71
^{40}A	275	1.19	327	98

*Values from Table 2.
**Average values obtained from value of k, Table 4.

Additional experiments with synchronized V79 cells were done with ^4He, ^7Li, ^{12}C, and ^{20}Ne ions. Survival data for ^{12}C and ^{20}Ne were reasonably reproducible for these experimental conditions. In Figure 14, age-responses of synchronized cells irradiated with ^4He, ^7Li, and ^{12}C ions are shown. The ^{12}C ion data are the average values of two such experiments with the standard deviation of the mean indicated.

Fig. 14 Age-response curves for irradiation of synchronized cultures with accelerated heavy ions as indicated in the figure.

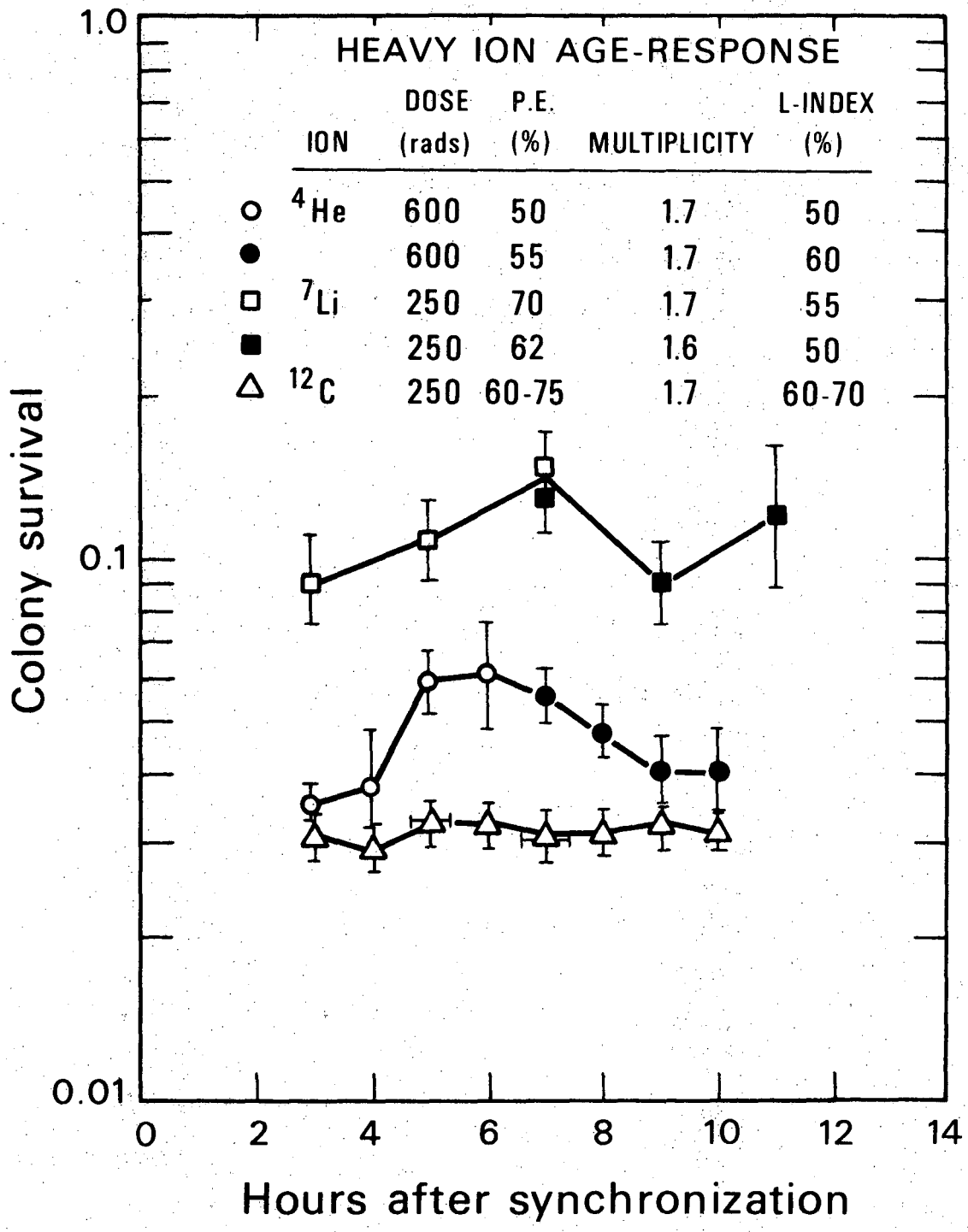
HEAVY ION AGE-RESPONSE
ION
DOSE (rads)
P.E. (%)
MULTIPLICITY
L-INDEX (%)
4He 600 50 1.7 50
600 55 1.7 60
7Li 250 70 1.7 55
250 62 1.6 50
12C 250 60-75 1.7 60-70
Colony survival
1.0
0.1
0.01
0
2
4
6
8
10
12
14
Hours after synchronization

DBL 719 5963

IV. DISCUSSION

A. High LET Radiation Age-Response

The results shown in Figures 8 and 14 demonstrate a variation in radiation sensitivity in the cell cycle for radiations of LET values from that of x-rays (2 KeV/micron) to that of lithium ions (43 KeV/micron). This variation has a similar time pattern for each type of radiation with the most resistant period in mid- to late- S phase. With radiations of very high LET (that of the carbon ions and greater) the age-response is apparently invariant. That is to say, within the limits of error in the experiments, there is no variation in the survival curves as the synchronized cell population progresses through the cell cycle.

The degree of cell-cycle variation that may be undetected in the very high LET radiation results can be estimated. Some individual data points have standard deviations of 20% to 30% although most points have lesser deviations. Survival curves perform an averaging process (assuming a smooth dose-response function) which reduces the allowable variation in the slope to the standard deviations indicated in Tables 3 and 4. In general, for these survival curves, the error in the slope is less than 5%. If the measured exponential curve consisted of two exponential curves representing different radiation responses, then this mixture should be detected readily if the responses differ by more than 20%. This estimate is graphically illustrated by Figure 15. The shaded areas in the top panel represent zones of experimental error (in this illustration a deviation in slope of 10% or at least twice the standard deviation). If the summation of the two radiation responses, weighted by their appropriate populations, extends outside this zone, the two are distinguishable. In the illustrated example, it was hypothesized that a synchronized population consisted of 80% of the cells with a unit negative slope and 20% with a negative slope of 0.8 at one time following synchronization. At a second time, there was a reversal in population distribution to 20% and 80% respectively. The two radiation responses are indicated as A and B in Figure 15. The resultant survival curves for the two times

Fig. 15 Graphical presentation, discussed in the text, of the possible, experimentally-masked variation in radiation response for heavy-ion irradiations.

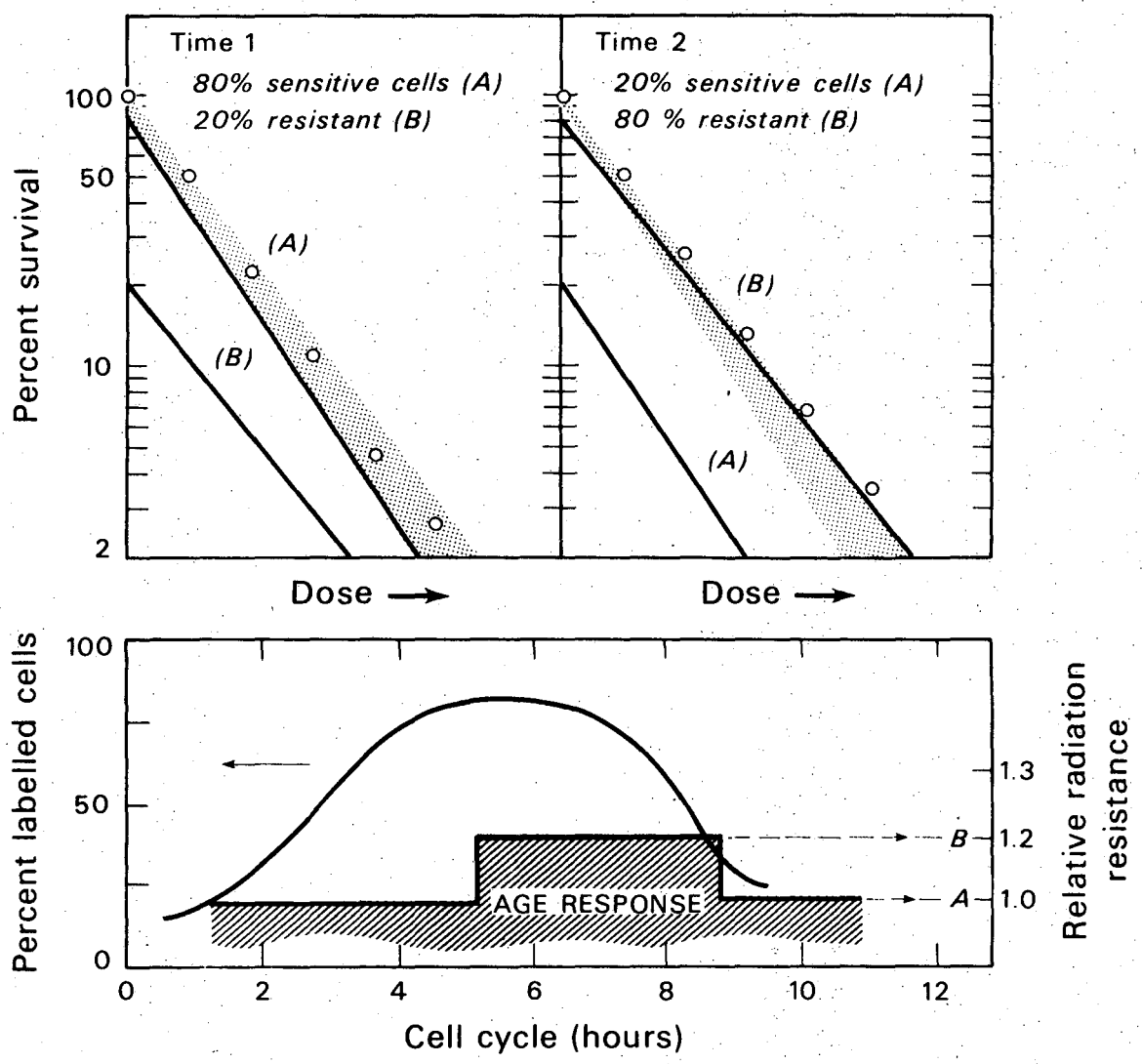
Time 1
80% sensitive cells (A)
20% resistant (B)
Time 2
20% sensitive cells (A)
80 % resistant (B)
Percent survival
100
50
10
2
(A)
(B)
(B)
(A)
Dose →
Dose →
Percent labelled cells
100
50
0
AGE RESPONSE
B
A
1.3
1.2
1.0
Relative radiation resistance
0
2
4
6
8
10
12
Cell cycle (hours)

DBL 719 5966

are indicated in the upper panel by the open circles. This example indicates the limit of distinguishable mixed populations for the 10% deviation in slope. It corresponds to a realistic degree of synchrony as indicated in the lower panel of Figure 15. The hypothesized populations correspond to a labeling index of 60% since the variation in the hypothesized age-response corresponds to sensitive G1 and early S cells (first survival curve) progressing to resistant late S cells (second survival curve) as schematically indicated. If the subpopulations had slightly different values of both D_{37} and extrapolation number (greater than the multiplicity value) such a combination could conceivably be more difficult to detect. Further analysis along this line has not been made.

The Chinese hamster cell age-response for different radiations can be compared from the results reported here and from the results of others. The radiation age-response is a variation in sensitivity as determined by the variation in surviving fraction when cells are exposed to the same dose of radiation at different cell-cycle used. Since different radiations are different in effectiveness, a comparison based on a common dose would be misleading. A comparison must be based on the biological effect which varies cyclically. Somewhat arbitrarily, the choice of surviving fraction for reference has been taken as that of G1 cells and the magnitude of variation from that sensitivity to the maximum survival (in late S) is referred to as the age-response amplitude. In this study, the age-response amplitude has the largest value for x-rays and no measurable amplitude for very high LET radiation. Thus, the effect of increasing LET on the age-response is to vary the amplitude from a large factor to a small factor. In order to compare results obtained for Chinese hamster cells by different investigators, the x-ray age-response amplitude can be normalized to 100%. Then, an invariant age-response would have a zero percent amplitude. In Figure 16, an attempt to compare the age-response as a function of LET is given. Ideally, the comparison should be made for irradiation, with both the test radiation and x-rays, of cultures from the same synchronized cell population. Some of the results

Fig. 16 The variation in survival, or age-response, for different radiations compared to that of x-rays. The closed circles are for results in this report; the open symbols are for results of others (referenced by number). The factor by which the late S cell survival is greater than the G1 cell survival is compared for the radiation LET of interest to that of x-rays when the respective doses used in the comparison yield the same G1 cell survival levels.

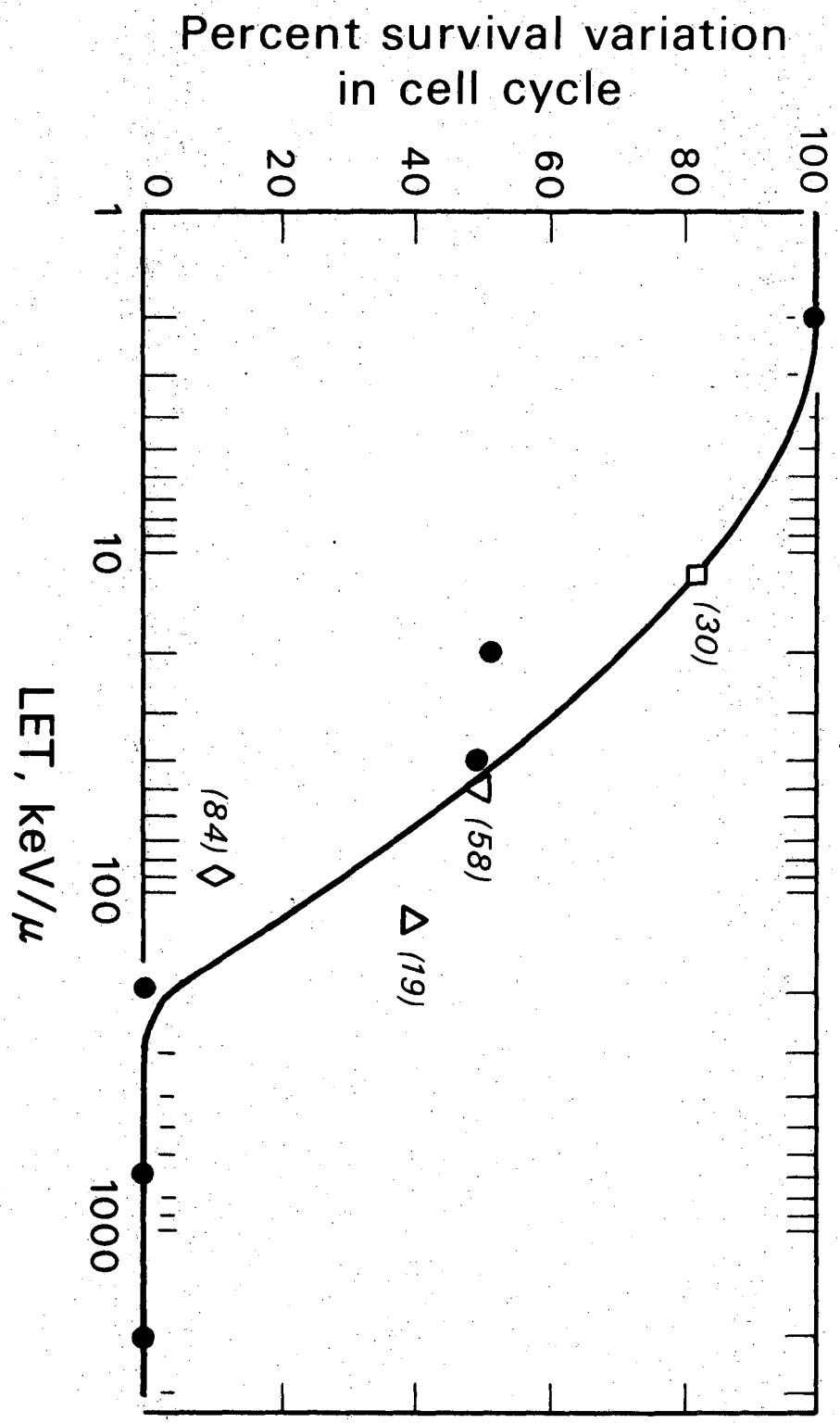

DBL 7111 6096

are compared directly with the x-ray response but other comparisons are made for average or typical age-responses. The closed circles are date determined from the experiments reported here, while the date of others is referenced accordingly. The "error bar" for the data of Skarsgard (included by Elkind in Ref. 19) reflects a lack of knowledge of what the corresponding (unpublished) x-ray age-response was. This approach to comparing age-response measurements, although certainly not the only possible approach, may be the simplest. It bases the comparison on cell-cycle times soon after the synchronizing procedure so that there is minimum loss of synchrony. This is particularly important for the sensitive cell-cycle time, G1 phase, in this study. However, the use of only two survival levels (maximum sensitivity and minimum sensitivity) requires adequate coverage of the cell cycle to clearly define those values. This simple approach is adequate when the shape of the age-response curve is not different for different radiations, a requirement apparently met with the Chinese hamster cell experiments reported here. The age-response amplitude simply diminishes with increasing LET. The similarity along the time axis of the age-response for different LET values suggests a change in the kind of damage rather than a change in damage site.

With haploid yeast cells, a similar effect of high LET radiation has been observed. The haploid yeast has been shown to have two radiation-response populations when irradiated with x-rays and alpha particles (20). The resistant population consists of cells with small buds when DNA synthesis is occuring (8,77). The sensitive cells have exponential survival curves, while the resistant, budding cells exhibit a broad-shouldered sigmoidal curve. Thus, the low LET survival curves do not correspond directly with the mammalian cell curves which are at least slightly sigmoidal at all cell-cycle times. However, with increasingly higher LET radiations, until a value between 100 and 200 KeV/micron, the difference in radiation response of these two subpopulations decreases (49). With the very high LET radiations the difference in survival is greatly reduced, but measurable. To the extent that the haploid yeast can

be compared to Chinese hamster cells, their age-response is effected similarly with increased LET values.

B. Application to Radiation Therapy

Heavy charged particles have been proposed for radiation therapy primarily because of their favorable depth-dose distribution. A given fluence of monoenergetic particles deposits the greatest dose at the Bragg peak (that is, at the highest LET value as the particles are slowed before charge neutralization reduces their LET). There is therefore a desirable "sparing" of the surface tissue and intermediate tissues while maximizing damage at a specific depth which would be the depth of a tumour. A second fact associated with the increased LET near the Bragg peak is the decreased effect of the presence of oxygen. This is an important consideration for radiation therapy in as much as there may be an anoxic population of viable tumour cells not as sensitive to low LET radiation as the normal, oxygenated tissues (an undesirable situation as pointed out in a different context by Bergonié and Tribondeau (9). Thus, the anoxic cells are killed on a par with oxygenated cells when irradiated with a sufficiently high LET radiation. These and other advantages of heavy charged particles for radiation therapy of localized tumours have been reviewed (69). These advantages apply in part (but to different degrees) to the proposed application of neutrons or negative pi-mesons for radiation therapy.

Knowledge of the low LET age-response could be used to advantage in radiation therapy although the complexities with low LET radiation are substantial (66). Following a dose of radiation, the surviving cells will be primarily those in a radioresistant phase. This obviously applies to both normal and tumour cells. The surviving fraction will depend on the percentage of such radioresistant cells in the tissue. Thus, radiation tends to produce a synchronized, surviving population. Any attempt to take advantage of a subsequent radiosensitive phase, in timing a series of exposures used in therapy, would necessarily require consideration of both normal and tumour cell repopulation and the relative frac-

tions of radiosensitive cells in these proliferating systems. That is to say, the necessary consideration of the relative sensitivity of normal and tumour cells must be applied to the regrowth of these populations. With very high LET radiation, the cell cycle is not a significant factor. Surface or intermediate tissues may have some cyclic variation because of the lower LET radiation "seen" by these tissues for the initial, impinging particles. The use of heavy charged particles would ensure that the normal and tumour cells would at least be on a par with regard to cyclic variations in sensitivity for any series of treatment exposures. In brief, the application of heavy charged particles to radiation therapy, in addition to other virtues, would ensure that the relative sensitivities of normal and diseased tissues would not be unfavorable throughout a course of exposures. The normal tissues would conceivably be less effected with an approppriate treatment schedule including low and high LET radiation treatments.

C. Comparison of Inactivation and Nuclear Cross-Sections

The nuclei of cells may be expected to double in volume over the cell cycle as does the cell volume (62). A doubled volume would result in a cross-sectional increase by a factor of 1.6. Measured nuclear cross-sections are compared in Figure 17 with that expected on the basis of a doubled volume, assuming a linear increase in volume with time. The trend of the results is reasonable except for the earliest cell-cycle time. This exception is probably due to the fact the cells are still quite round in the G1 phase following shake-off. That is to say, the trend of measured cross-sectional growth is for a flattened cell nucleus, with an enhanced increase in cross-section due to the flattening process in the first hour or so after inoculating cells into cultures. An experiment in which excessively vigorous shaking was used resulted in a high yield of cells, poor synchrony, and broad distributions of nuclear cross-sections at different times after shaking. Yet, a significant rise in cross-sectional area of the nucleus occurred in the first two hours suggesting significant flattening of the nucleus in that time as the cell reattached and flattened.

Fig. 17 Comparison of inactivation cross-sections and cross-section measurements of V79 cell nuclei. The circles are average nuclear cross-sections reproduced from Figure 6. The dashed curve is a hypothesized nuclear cross-section growth curve assuming the volume of the nucleus doubles linearly with cell-cycle time: area $\propto$ (volume)$^{2/3}$ $\propto$ (time)$^{2/3}$. The inactivation cross-sections for carbon, neon, and argon ions are diagrammed as cell-cycle invariant values.

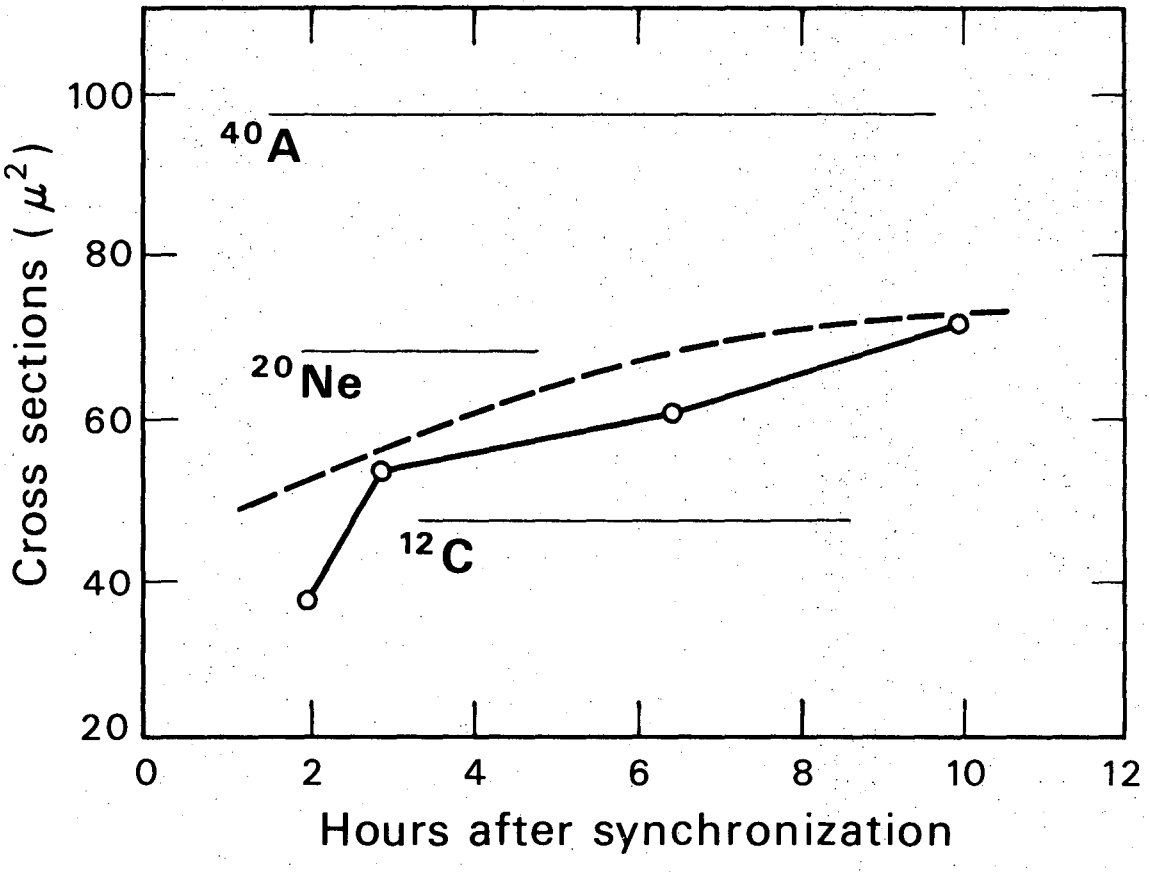

DBL 725 5314

The effect of flattening is apparent in Figure 3 where the nuclei of flattened cells have larger cross-sections than the two rounded cells (identified by their phase contrast "halo" in Panel A) that are probably early G1 cells.

Figure 17 also compares the cell nuclear cross-section at different cell-cycle times to the inactivation cross-sections (see Table 5). The closeness of agreement between early cell-cycle times and the calculated cross-section based on carbon ion and neon ion irradiation is noteworthy, as discussed in the introduction. Yet, while the biological cross-section changes substantially, the inactivation cross-section does not. It is tempting to consider the whole nucleus as sensitive and suggest an increasing resistance with cell-cycle progress. However, this would require a change in survival curve either as slope or as extrapolation number, the latter implying that on the average more than one ion is required per nuclear area for killing during the late portions of the cell cycle. Neither of these changes is indicated substantially in the survival curves after accounting for cell multiplicity. A second possibility would be an increased density of the nucleus with cell "age" which would alter the actual absorbed dose from one age to another. However, a change in density of the magnitude necessary is highly unlikely, especially in light of the increased nuclear volume.

The inactivation cross-section data for carbon, neon, and argon ions thus indicate a radiosensitive volume that is constant at least in the two dimensions of its cross-sectional area. In contrast, the nuclear cross-section increases substantially. The whole nucleus is therefore <u>not</u> implicated at all cell ages as a uniformly sensitive volume.

For argon ions, the inactivation cross-section is larger than that of the cell nucleus. This point is discussed further in subsection IVD.2. First, the accuracy of the inactivation cross-section values will be considered. There are two questions of concern: The absolute inactivation cross-section for a given ion and the observed trend of increasing cross-section for increasing values of high LET. The minimum requirement for determining the

inactivation cross-section would be a measurement of the number of particles per unit sample area. This must also be related to the LET value of the beam which is ideally uniform and monoenergetic. The system for absolute dosimetry, described in Section II and elsewhere (40,70,73), uses an ionization chamber to determine the absorbed dose rather than determining the particle fluence. The conversion from absorbed dose to particle fluence is based on the physical properties of the accelerated ions (40,50) and calibration of the chamber against both an x-ray machine (70) and a helium ion fluence measured by a Faraday cup (40). The ionization chamber was designed for absolute dosimetry (i.e., small electrode spacing and high collecting voltage to minimize ionic recombination). In support of its use for relating dose to particle fluence, the dosimetry system used at the Yale HILAC can be mentioned. There, an ionization chamber is used as a monitor and nuclear track emulsion is used for absolute dosimetry by measuring the particle fluence. The doses evaluated separately from these independent Yale detectors were noted (73) to be within 5% of each other. It is therefore expected that the Berkeley ionization chamber can be used to determine the particle fluence with a similar accuracy.

The increase of inactivation cross-section with increasing LET (carbon ion to argon ion) could arise as a systematic error in dosimetry in different ways: if the value of the energy loss per ionization event decreased with increasing LET; if ion recombination along the particle track increased with increasing LET; if the beam were inadequately scattered (non-uniform) with carbon ions and more uniformly scattered for higher LET ions; or if the dose correction factor were increasingly too small for increasing LET.

The first two items concern the efficacy of the ionization chamber measurement for determining particle fluence which was just discussed. Further, the value of energy per ionizing event is not expected to vary sufficiently to account for the variation of inactivation cross-section and is known to be essentially constant between proton and alpha-particle measurements. Although

recombination along the ion track has been of concern for measuring densely ionizing particles with ionization chamber (65), it apparently is not a significant factor as indicated by voltage saturation measurements (70, 73) and by the Yale dosimetry comparison. The third item, concerning uniformity of the beam over the sample area, could be significant if the carbon ion beam were most intense in the center of the sample. This arrangement would be the least efficient per fluence for inactivating cells. However, for both carbon and argon ions, the distribution of cells in the irradiation dish was different in different experiments. For a one millimeter inoculum, the cells were distributed over the culture dish bottom, but with one-half millimeter inoculum, cells were intentionally restricted to be centrally concentrated. The survival results did not vary significantly in the two situations. The fourth item, concerning dose correction factors is considered insignificant because of the close agreement of measured and calculated Bragg curves. That is to say, lower energy particles "contaminating" the beam as a result of scatter could give a Bragg ratio, between the ionization chamber and sample positions, altered from the theoretical which was not observed. Also, such an effect would probably not be systematic with LET. These considerations do not suggest a significant dosimetry error associated with the inactivation cross-section values.

D. Interpretations

1. High LET Trends

Figure 9 demonstrates with asynchronous cultures that there is a radiation LET value that is most effective for inactivation of mammalian cells. Such an observation has been made with different biological systems and different criteria of dose-response as cited in the introduction. When survival curves are exponential for all the LET values, this peak efficiency in LET may be interpretable in terms of the probability factor, p (L), of Equation 4 such that as L increases to large values, p (L) increases toward a value of unity. Recently, analyses have been applied to the case of mammalian cells including the range of LET values in which the survival curve shape changes for single cell inactiva-

tion. Barendsen (4) interpreted his sigmoidal survival curve data assuming that the initial negative slope, for each LET value, is due to lethal events of the same kind. With increasing LET the observed initial slopes are increasingly steep until exponential curves are obtained. Thus, one part of sigmoidal curves is compared with the slope of the exponential survival curves. Alternatively, the slope of the high dose (exponential) region of sigmoidal survival curves has often been used to compare radiation sensitivities.

Todd (70) modeled his mammalian cell experimental data for various LET radiations according to the product of two factors: an exponential factor and a sigmoidal factor (multi-target form). The mean lethal dose for each factor was used to calculate its inactivation cross-section as a function of LET. These two factors were considered to correspond to two kinds of damage (in his terminology reversible and irreversible) the proportion of the two changing with LET such that the very high LET radiation produces practically all irreversible damage as suggested in his dose-fractionation experiments (72).

Recently, Tobias (68) reviewed the high LET trends for lethality of several different biology systems and fitted the LET dependence of the probability factors to a general form interpreted as containing two modes of lethality, one due to a single ionization event and the second due to cooperative action between ionizations produced closely together along the charged particle track.

These models for high LET radiation killing were applied to results obtained for exponentially growing mammalian cell cultures. The results reported here are, for low LET radiations, an age-response variation of the inactivation cross-section (when defined as the high dose slope) and, with increasing radiation LET, a decreasing age-response. The magnitude of the low LET variation is small when considering the range of inactivation cross-sections. The age-response can be considered as a perturbation on the models; for example, as a damage repair probability. Figure 16 is

an estimate of such an age-dependent "perturbation" as a function of LET.

Each of the above models includes at least two kinds of damage or damage sites. Also, each assumes a limiting cross-section for sufficiently large LET values. In Figure 17 and subsection IV.C., the inactivation cross-sections determined for the three very high LET ions are compared showing that there is a substantial increase over this range of LET values. In the following subsection, two possible explanations for the increase are considered. However, it is worthwhile to note that this phenomenon of increasing inactivation cross-section at these highest LET values has been reported (e.g. Ref. 40). In particular, the data of Todd (70) with a human cell line and of Skarsgard (63) with a Chinese hamster cell line show this phenomenon (see Table I).

2. Argon-ion Results

The simplest interpretation of an increasing inactivation cross-section is that the probability factor, p (L), has not reached saturation. Comparison of the inactivation cross-section with the measured nuclear cross-sections, Figure 17, indicates that with such an interpretation the cytoplasm would be sensitive to the argon ions. However, this is not expected since the cytoplasm has been found to be very resistant to different radiations, including α-particles (as cited in the Introduction). The possibility exists that a different kind of lethality is occuring at very high LET values, one which would involve not just the nucleus but perhaps the whole cell. This possibility has not been investigated.

Comparison of these very high LET results with another biological system suggests that the increased cross-section is not necessarily a consequence of an increasing probability factor. Figure 18 compares the inactivation cross-sections as a function of LET for a non-dividing mammalian cell system, lymphocytes, (as measured by Madhvanath (40)). These measurements were made with the Berkeley HILAC with practically the same dosimetry conditions

Fig. 18 Comparison of the target cross-sections determined by Madhvanath (53) for human lymphocytes and for V79 cells. The dashed portion of the V79 cells curve was determined from the high-dose slope of sigmoid survival curves. The average, total lymphocyte cross-section was 40 μ^2.

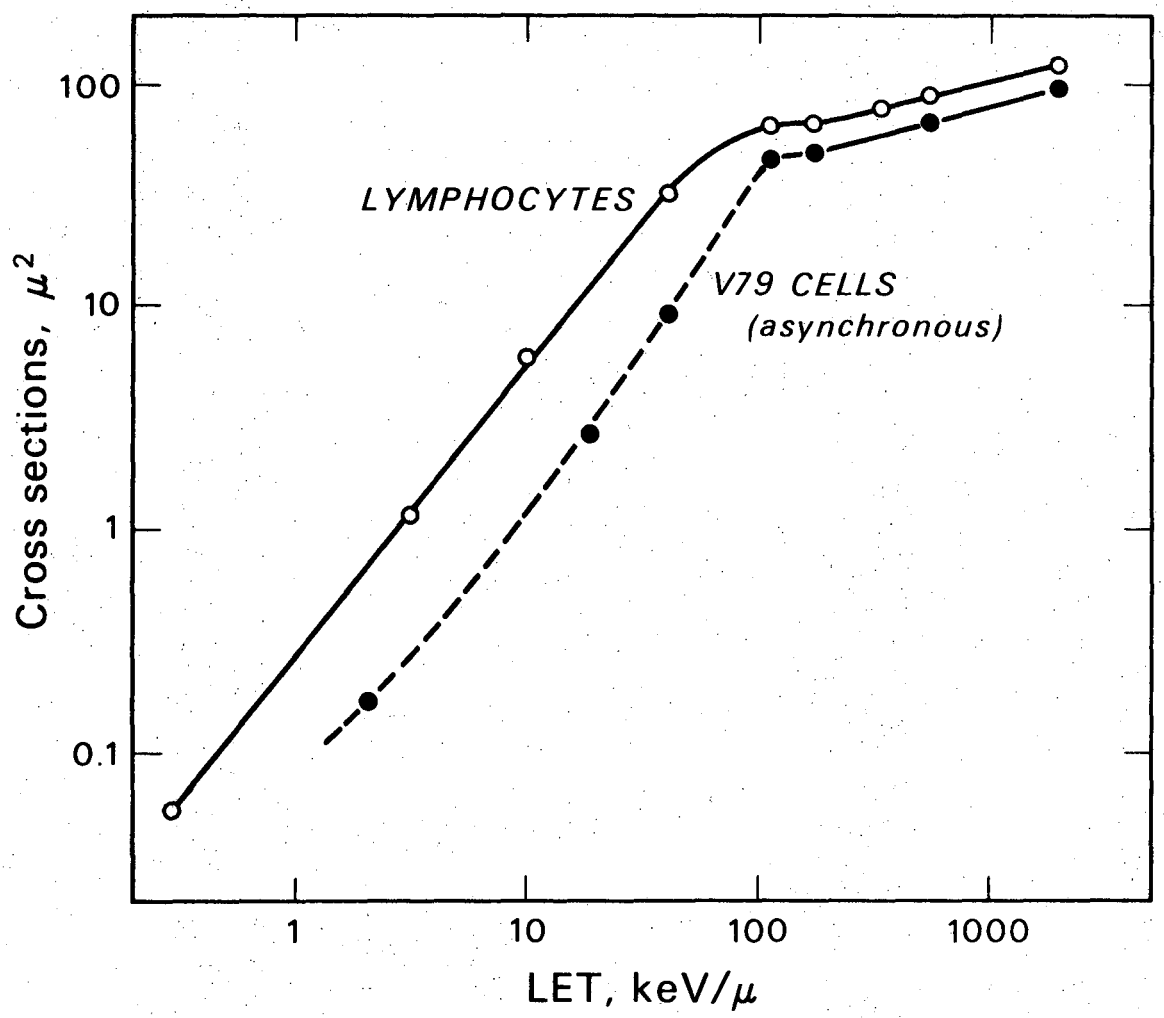

DBL 7111 6098

and often concurrently with the same ion beam. Clearly, the lymphocytes are more sensitive to radiation but in the region of very high LET values the trends of inactivation cross-sections are very similar. The lymphocyte inactivation cross-sections for LET values greater than 100 KeV/micron are larger than the average lymphocyte cell cross-section. This result implies a substantial role for secondary electrons. It also suggests that with proliferating mammalian cells, the role of secondary electrons produced by very high LET radiations may be significant. The parallel trends between the very high LET inactivation cross-section of lymphocytes and Chinese hamster cells could also suggest a similar kind of damage mechanism in both systems. The concensus of opinion seems to be that the site of lethal damage in non-dividing lymphocytes is the cell membrane. The parallel for Chinese hamster cells might then be the nuclear membrane as the site for very high LET radiations. This is reminiscent of the theory of Alper (1). However, the inactivation cross-section does <u>not</u> reflect a change like that of the increasing nuclear cross-section.

There has often been consideration given to the role of secondary electrons and whether their contributed ionization should be excluded in dose-response relations or in the defnition of LET (24, 33, 38). Attempts to observe an effect due to secondary electrons have compared the response of mammalian cells to heavy ions of the same LET value but with differing charges and velocities (40, 70). Such a comparison attempts to observe a difference due to the altered dose contribution of the secondary electrons. The results reported have not shown a significant difference. However, the range of LET values used in the studies did not include values as high as that of argon ions. Cole (15) has measured the range of low-energy electrons in air and in plastic (collodion). For normal incidence, the range (1% ionization transmission) of 7 KeV electrons was then estimated for water to be 1.7 microns, which corresponds to the difference in radius of two circles corresponding in area to the carbon and argon inactivation cross-sections. Electrons of this and higher energy account for only a few percent of the total dose (24) so that a biological ef-

fect at such a radius is expected to be slight.

Recently, Katz and colleagues (36) have produced a mathematical model for survival curves of different cells. It accomodates a change in survival curve shape for increasing LET (although it does not accomodate a peak LET efficiency when the survival curves are all exponential). Interestingly, this model also accomodates an increase in the very high LET inactivation cross-sections approximately to the extent indicated in Figure 17. This is the consequence in the model of secondary electrons produced in sufficient number and range to overlap at the necessary radius and produce an ionization density sufficient to cause the biological effect. This phenomenon would be present, also, with the carbon ions such that the inactivation cross-section is approximately 40% larger than a hypothesized biological cross-section. Thus, for the argon ion irradiation, the biologically effective range of secondary electrons, according to this model, would be greater than estimated above as 1.7 microns and would be approximately 2.2 microns. The ionization density at this radius is large enough, according to the model, to produce biologically a very high LET effect. Very high LET irradiation of mammalian cells measuring the oxygen effect (5,70) and the age-response require that the fraction of cells killed by a low LET component of radiation is small.

Further studies of the secondary-electron contribution to radiation biology are necessary to test this new emphasis placed on them by the models of Katz, et.al. (12,36). Measurements of micro-radial distributions of dose and LET are being made for protons and alpha particles at Brookhaven National Laboratory (85). Extension of these measurements to higher LET radiations and more detailed calculations of the radial distributions for secondary electrons (13) will be of interest to further interpretations of the results reported here.

3. Speculations

Recent radiobiology results with yeast suggest that the cell-cycle variation in sensitivity is due to a variation in repair of

damage. Resnick (51) isolated x-ray sensitive mutants of haploid yeast whose increased sensitivity was due mainly to an altered response of the cells with small buds. These cells normally exhibit a sigmoidal survival curve with a substantial "shoulder" in contrast to the other cells with an exponential survival curve. In the mutants, the cells with small buds do not exhibit the difference in radiation response from the rest of the population. Genetic studies suggested to Resnick that such a mutant was defective in its ability to enzymatically alter radiation damage. The lack of cyclic variation in the mutant radiosensitivity to x-rays can be compared to the greatly reduced cyclic variation of wild type haploids irradiated with very high LET radiation (49). This suggests that the high LET radiation damage is not susceptible to enzymatic repair. The similar LET dependence of the age-response may be due to variation in a repair capability. This implication is in line with the contention of Elkind (19) that the "shoulder" of a sigmoidal survival curve reflects directly the repair of some radiation damage, as mentioned in the Introduction. With this hypothesis, the proportions of different kinds of low LET radiation damage may be susceptible to cell cycle variation, or the conditions for repair or availability of repair enzyme may vary.

The kind of radiation damage most often suggested as causing lethality is double-strand breakage of DNA. Recent experiments on the production of double-strand breaks as a function of the LET of the radiation afford an opportunity to make a comparison of cell lethality and DNA double-strand breaks. Christensen (14) irradiated the replicated form of ϕX-174 viral DNA, which is double-stranded in this form, with various radiations including heavy ions accelerated at the Berkeley HILAC. Figure 19 compares the target cross-section for double-strand breaks with the target cross-section of V79 cells as a function of LET. Again, the result for V79 cells include the high dose slopes in the case of sigmoidal survival curves. The closeness of the two trends up to the size of the nucleus is remarkable. The ϕX-174 DNA was irra-

Fig. 19 Comparison of the target cross-sections for V79 cells (as in Figure 18) and the action cross-sections for radiation induced double-strand breaks in replicative form ϕX-174 DNA determined by Christensen (14).

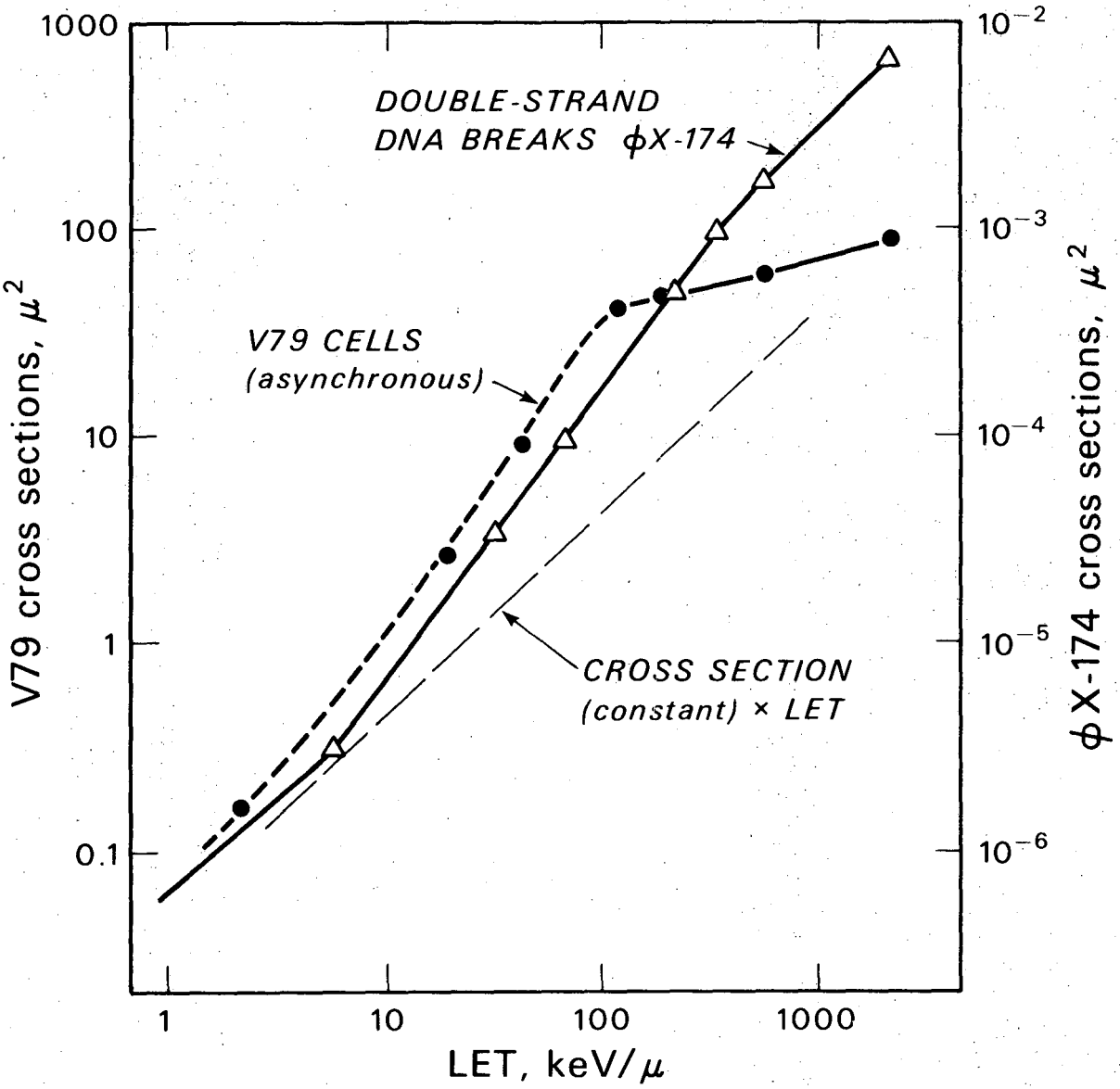

DBL 7111 6097

diated in a protective broth to minimize "indirect" damage. Comparison with Chinese hamster cells therefore must be carefully qualified. Yet, the fact that DNA double-strand breakage increases above the line of proportionality between cross-sections and LET is itself highly significant. One can speculate that the very high LET damage in mammalian cells that is independent of the cell cycle, independent of chemical modifiers, and not repairable is DNA double-strand breakage arising from cooperative events along the heavy ion track. This kind of damage would be included in the low LET irradiations as largely reflected by the D_0 of the survival curves.

E. Summary

The major result of this study is the direct determination that the Chinese hamster cell age-response is LET dependent. At sufficiently high LET values, the age-response is invariant and therefore apparently not related to cell-cycle "growth" of the nuclear cross-section. Further, these LET studies of the cell cycle provide no evidence to exclude the idea of one kind of structure or molecule sensitive to low and high LET radiations.

The results with very high LET radiations indicate a further potential advantage of such radiations in radiation therapy applications. The use of very high LET radiation could ensure a favorable relation between the radiosensitivities of normal and diseased tissues throughout a course of radiation treatments.

Although the very high LET results provide values of inactivation cross-sections, interpretation of these values in terms of biological cross-section is made difficult by the uncertainty in the contribution of secondary-electrons to the cross-section. However, it is reasonable to interpret the results as implicating a biological cross-section nearly as large as the nucleus of the cell early in the cell cycle. The results reported here show a constant inactivation cross-section during the increase in nuclear cross-section, suggesting that the nucleus is non-uniform in its sensitivity to very high LET radiation.

ACKNOWLEDGEMENTS

This research was performed under the auspices of the US Atomic Energy Commission and was aided by support from NASA. As a student, I was support d first by a USAEC Special Fellowship in Health Physics and then a NIH Biophysics Training Grant fellowship. I am grateful to those who sponsored these fellowships. The support of the HILAC irradiations by Prof. C.A. Tobias is also gratefully acknowledged.

The advice and enthusiasm of Dr. Jack Burki were invaluable during the course of this research. I wish to express many thanks to him. I also wish to thank a colleague, Dennis Ross, for the many discussions, suggestions, and assistance contributed by him. Numerous others provided encouragement and stimulating discussions as well. My initial interest in high LET radiation studies was stimulated by the lectures of Dr. G.M. Barendsen as a visiting professor. The interest of Dr. Warren Sinclair in this particular project was encouraging to me, and his contribution of the V79 subline cells and synchrony method is acknowledged and appreciated.

Technical assistance was ably given by many people at crucial steps in this effort. The staff at Donner Laboratory in general, the initial culturing demonstrations and continued assistance of Mrs. K. Lathrop, and the indispensable assistance with HILAC measurements by Mr. Jerry Howard and Dr. Udipi Madhvanath are all gratefully acknowledged.

This report could not have been produced without the sustained assistance of Mrs. Linda McColgan to whom I am deeply grateful. The forebearance of my family and the stamina and support of my wife were essential in the completion of this endeavor.

REFERENCES

1. T. Alper, Mechanisms of lethal radiation damage to cells in Proceedings of the Second Symposium on Microdosimetry (1969) H.G. Ebert, Ed. (Commission of the European Communities, Brussels, 1970).

2. S. Bachetti and W.K. Sinclair, The effects of x-rays on the synthesis of DNA, RNA, and proteins in synchronized Chinese hamster cells. Radiation Res. 45, 598-612 (1971).

3. G.W. Barendsen, Possibilities for the application of fast neutrons in radiotherapy: recovery and oxygen enhancement of radiation-induced damage in relation to linear energy transfer, Europ. J. Cancer 2, 333-345 (1966).

4. G.W. Barendsen, Mechanism of action of different ionizing radiations on the proliferative capacity of mammalian cells, in Theoretical and Experimental Biophysics Vol. 1, A. Cole, Ed. (Marcel Dekker, Inc., New York, 1967).

5. G.W. Barendsen, C.J. Koot and G.R. van Kersen, The effect of oxygen on impairment of the proliferative capacity of human cells in culture by ionizing radiations of different LET. Int. J. Radiat. Biol. 10, 317-327 (1966).

6. G.W. Barendsen and H. Walter, Effects of different ionizing radiations on human cells in tissue culture IV. Modification of radiation damage. Radiation Res. 21, 314-329 (1964).

7. G.W. Barendsen, H.M.D. Walter, J.F. Fowler, and D.K. Bewley, Effects of different ionizing radiations on human cells in tissue culture III. Experiments with cyclotron-accelerated alpha particles and deuterons, Radiation Res. 18, 106-119 (1963).

8. C.A. Beam, R.K. Mortimer, R.G. Wolfe and C.A. Tobias, The relation of radioresistance to budding in S. Cerevisiae. Arch. Biochem. Biophys. 49, 110-122 (1954).

9. J. Bergonié and L. Tribondeau, Interprétation de quelques résultats de la radiothérapie et essai de fixation d'une technique rationnelle, C.R. Acad. Sci. Paris 143, 983-985 (1906).

10. L.K. Blumenthal and S.A. Zaler, Index for measurement of synchronization of cell populations. Science 135, 724 (1962).

11. H.J. Burki and S. Okada, A comparison of the killing of cultured mammalian cells induced by decay of incorporated tritiated molecules at -196° C. Biophys. J. 8, 445 (1968).

12. J.J. Butts and R. Katz, Theory of RBE for heavy ion bombardment of dry enzymes and viruses. Radiation Res. 30, 855-871 (1967).

13. A. Chatterjee, Stopping power, range, and penetration of low-energy electrons in water. (Ph.D. thesis, 1971) University of Notre Dame.

14. R.C. Christensen, Heavy-ion-induced single- and double-strand breaks in ϕX-k74 reokucatuve form DNA. (Ph.D. thesis, 1971) LBL-28, Lawrence Berkeley Lab., Univ. of Calif., Berkeley.

15. A. Cole, Absorption of 20eV to 50,000 eV electron beams in air and plastic, Radiation Res. 38, 7-33 (1969).

16. R.A. Deering and R. Rice, Jr., Heavy ion irradiation of HeLa cells, Radiation Res. 17, 774-786 (1962).

17. H. Dertinger and H. Jung, Molecular Radiation Biology, (Springer-Verlag, New York, 1970).

18. W.C. Dewey and R.P. Thompson, Distribution of DNA in Chinese hamster cells. Exptl. Cell Res. 48, 605-617 (1967).

19. M.M. Elkind, Damage and repair processes relative to neutron (and charged particle) irradiation, in Current Topics in Radiation Research, Vol. VII, M. Ebert and A. Howard, Eds. (North-Holland Publ. Co., Amsterdam, 1970).

20. M.M. Elkind and C.A. Beam, Variation of the biological effectiveness of x-rays and α-particles on haploid S. Cerevisiae. Radiation Res. 3, 88-104 (1955).

21. M.M. Elkind and H. Sutton, Radiation response of mammalian cells grown in culture I. Repair of x-ray damage in surviving Chinese hamster cells. Radiation Res. 13, 556 (1960).

22. M.M. Elkind and G.F. Whitmore, The Radiobiology of Cultured Mammalian Cells, (Gordon and Breach Science Publishers, New York, 1967).

23. J. Engleberg, A method of measuring the degree of synchronization of cell populations. Exp. Cell Res. 23, 218 (1961).

24. D.J. Fluke, T. Brustad and A.C. Birge, Inactivation of dry T-1 bacteriophage by helinm ions, carbon ions, and oxygen ions: Comparison of effect for tracks of various ion density. Radiation Res. 13, 788-808 (1960).

25. D.K. Ford and G. Yerganian, Observations on the chromosomes of Chinese hamster cells in tissue culture. J. Nat. Cancer Inst. 21, 393 (1958).

26. P.H. Fowler and D.H. Perkins, The possibility of therapeutic applications of beams of negative pi mesons, Nature 189, 524-528 (1961).

27. H. Fricke and E.J. Hart, Chemical dosimetry, in Radiation Dosimetry, Vol. II, F.H. Attix, W.C. Roesch, and E. Tochilin, Eds. (Academic Press, New York, 1966).

28. W.D. Gude, Autoradiographic Techniques (Prentice-Hall, Inc., Englewood Cliffs, N.J., 1968).

29. G.M. Hahn, Radiobiology of mammalian cells in the plateau phase of growth, in Time and Dose Relationships in Radiation Biology as Applied to Radiotherapy, V.P. Bond, H.D. Suit and V. Marcial, Eds. 117-129 (Report BNL 50203 (C-57), 1969).

30. E.J. Hall, Radiobiological measurements with 13 Mev neutrons. Brit. J. Radiol. 42, 805 (1969).

31. E.J. Hall, Cell killing at very low dose rates, in Time and Dose Relationships in Radiation Biology as Applied to Radiotherapy, 308-317 (Report BNL 50203 (C-57), 1969).

32. P. Howard-Flanders, Physical and chemical mechanisms in the injury of cells by ionizing radiations, Advan. Biol. Med. Phys. 6, 553 (1958).

33. International Commission on Radiological Units and Measurements, Radiation Qualities and Units, ICRU Report No. 16 (1970).

34. H.S. Kaplan, Radiobiology's contribution to radiotherapy: promise or mirage? Radiation Res. 43, 460-476 (1970).

35. H.S. Kaplan and L.E. Moses, Biological complexity and radiosensitivity, Science 145, 21 (1964).

36. R. Katz, B. Ackerson, M. Homayoonfar, and S.C. Sharma, Inactivation of cells by heavy ion bombardment, Radiation Res. 47, 402-425 (1971).

37. J. Kruuv and W.K. Sinclair, X-ray sensitivity of synchronized Chinese hamster cells irradiated during hypoxia. Radiation Res. 36, 45-54 (1968).

38. D.E. Lea, Actions of Radiations on Living Cells, 2nd ed. (Cambridge Univ. Press, New York, 1955).

39. G.M. Litton, J. Lyman, and C.A. Tobias, Penetration of High-Energy Heavy Ions, with the Inclusion of Coulomb, Nuclear, and Other Stochastic Processes. Lawrence Radiation Laboratory report UCRL-17392 Rev., 1968.

40. U. Madhvanath, Effects of Densely Ionizing Radiations on Human Lymphocytes Cultured in vitro. (Ph.D. thesis, 1971), Lawrence Radiation Laboratory report UCRL-20680.

41. D. Morkovin and A. Feldman, End point of one of the actions of radiations on living tissue important in radiation therapy and in acute radiation syndrome. Brit. J. Radiol. 33, 197 (1960).

42. R.K. Mortimer, T. Brustad, and D.V. Cormack, Effectiveness of ionizing radiations for induction of mutations and lethality in diploid Saccharomyces Cerevisiae in relation to ionization density and oxygen tension, Radiation Res. 26, 465 (1965).

43. T.R. Munro, The relative radiosensitivity of the nucleus and cytoplasm of Chinese hamster fibroblasts. Radiation Res. 42, 451-470 (1970).

44. S. Okada, Radiation Biochemistry, Vol. I: Cells, K. Altman, G. Gerber, S. Okada, Eds. (Academic Press, New York, 1970).

45. D.F. Peterson, E.C. Anderson, and R.A. Tobey, Mitotic cells as a source of synchronized cultures, in Methods in Cell Physiology, Vol. III, D.M. Prescott, Ed. (Academic Press, New York, 1968).

46. E.L. Powers, J.T. Lyman, and C.A. Tobias, Some effects of accelerated charged particles on bacterial spores, Int. J. Radiat. Biol. 14, 313-330 (1969).

47. T.T. Puck and P.I. Marcus, Action of x-rays on mammalian cells. J. Exptl. Med. 103, 653-666 (1956).

48. E.M. Pugh and G.H. Winslow, The Analysis of Physical Measurements, (Addison-Wesley Publishing Co., Reading, Mass., 1966).

49. M.R. Raju, M. Gnanapurani, B. Stackler, U. Madhvanath, J. Howard, J.T. Lyman, T.R. Manney and C.A. Tobias, Influence of linear energy transfer on the radioresistance of budding haploid yeast cells. (Manuscript in preparation).

50. M.R. Raju, J.T. Lyman, T. Brustad, and C.A. Tobias, Heavy charged-particle beams, in Radiation Dosimetry, Vol. III, F.H. Attix, W.C. Roesch and E. Tochilin, Eds. (Academic Press, New York, 1969).

51. M.A. Resnick, Genetic Control of Lethality and Mutation in Saccharomyces Cerevisiae. (Ph.D. thesis, 1968). Lawrence Radiation Laboratory report UCRL-18404.

52. E. Robbins and P.I. Marcus, Mitotically synchronized mamalian cells: A simple method of obtaining large populations. Science 144, 1152-1153 (1964).

53. D.W. Ross and W.K. Sinclair, Cell cycle compartment analysis of Chinese hamster cells in stationary phase cultures. Cell and Tissue Kinetics 5, 1 (1972)

54. John Seed, Studies of biochemistry and physiology of normal and tumour strain cells. Nature 198, 147-153 (1963).

55. W.K. Sinclair, Hydroxyurea: Effects on Chinese hamster cells grown in culture. Cancer Res. 27, 297-308 (1967).

56. W.K. Sinclair, Cyclic x-ray responses in mammalian cells in vitro. Radiation Res. 33, 620-643 (1968).

57. W.K. Sinclair, Protection by cysteamine against lethal x-ray damage during the cell cycle of Chinese hamster cells. Radiation Res. 39, 135-154 (1969).

58. W.K. Sinclair, Dependence of radiosensitivity upon cell age, in Time and Dose Relationships in Radiation Biology as Applied to Radiotherapy, V.P. Bond, H.D. Suit and V. Marcial, Eds. p. 97-116. (Report BNL 50203 (C-57), 1969).

59. W.K. Sinclair, Methods and criteria of mammalian cell synchrony, in Normal and Malignant Cell Growth, Recent Results in Cancer Research, 17 (Springer-Verlag, New York, 1969).

60. W.K. Sinclair and R.A. Morton, Variations in x-ray response during the division cycle of partially synchronized Chinese hamster cells in culture. Nature 199, 1158 (1963).

61. W.K. Sinclair and R.A. Morton, X-ray sensitivity during the cell generation cycle of cultured Chinese hamster cells. Radiation Res. 29, 450-474 (1966).

62. W.K. Sinclair and D.W. Ross, Modes of growth in mammalian cells. Biophys. J. 9, 1056-1070 (1969).

63. L.D. Skarsgard, B.A. Kihlman, L. Parker, C.M. Pujara, and S. Richardson, Survival, chromosome abnormalities, and recovery in heavy-ion and x-irradiated mammalian cells. Radiation Res. Supplement 7, 208-221 (1967).

64. A.H. Sparrow, A.G. Underbrink, and R.C. Sparrow, Chromosomes and cellular radiosensitivity. I. The Relationship of D_o to chromosome volume and complexity in seventy-nine different organisms, Radiation Res. 32, 915 (1967).

65. F.W. Spiers, Radiation units and theory of ionization dosimetry, in Radiation Dosimetry, G. Hine and G. Brownell, Eds. (Academic Press, New York, 1956).

66. G.G. Steel, The kinetics of cell proliferation in tumours, in Time and Dose Relationships in Radiation Biology as Applied to Radiotherapy, V.P. Bond, H.D. Suit, V. Marcial, Eds., 130-153 (Report BNL 50203 (C-57), 1969).

67. T. Terasima and L.J. Tolmach, Variations in several responses of HeLa cells to x-irradiation during the division cycle. Biophys. J. 3, 11-32 (1963).

68. C.A. Tobias, Physical energy transfer and biological effect, in Advances in Medical Physics, J. Laughlin, Ed. p 28-50. (Second International Congress on Medical Physics, August, 1969).

69. C.A. Tobias and P. Todd, Heavy charged particles in cancer therapy, in National Cancer Institute Monograph, 24: Conference on Radiobiology and Radiotherapy (U.S. Dept. of Health, Education, and Welfare, 1967).

70. P. Todd, Reversible and Irreversible Effects of Ionizing Radiations on the Reproductive Integrity of Mammalian Cells Cultured in vitro. (Ph.D. thesis) 1964. UCRL-11614, Lawrence Rad. Lab., U. of Calif., Berkeley.

71. P.W. Todd, Heavy-ion irradiation of cultured human cells. Radiation Res. Supple. 7, 196-207 (1967).

72. P. Todd, Fractionated heavy ion irradiation of cultured human cells. Radiation Res. 34, 378-389 (1968).

73. P.W. Todd, J.T. Lyman, R.A. Armer, L.D. Skarsgard, and R.A. Deering, Dosimetry and apparatus for heavy ion irradiation of mammalian cells in vitro. Radiation Res. 34, 1-23 (1968).

74. O.A. Trowell, Tissue culture in radiobiology, in Cells and Tissues in Culture, Chapt. 2, Vol. 3, E.N. Willmer, Ed. (Academic Press, London, 1966).

75. R. Tym and P. Todd, The sensitization by iododeoxyuridine of cultured human cells to the lethal effects of x-rays and heavy ions. Int. J. Radiat. Biol. 8, 589-603 (1964).

76. R.C. von Borstel, Effects of radiation on cells, in The Biological Basis of Radiation Therapy, E.E. Schwartz Ed. (J.B. Lippincott Co., Philadelphia, 1966).

77. D.H. Williamson, Nuclear events in synchronously dividing yeast cultures, in Cell Synchrony, I.L. Cameron and G.M. Padilla, Eds. (Academic Press, New York, 1966).

78. A. Zermeno and A. Cole, Radiosensitive structure of metaphase and interphase hamster cells as studied by low-voltage electron beam irradiation. Radiation Res. 39, 669-684 (1969).

79. E. Zenthen, Artificial and induced periodicity of living cells. Advances Biol. and Med. Physics 6, 37 (1958).

80. K.G. Zimmer, Studies on Quantitative Radiation Biology (Oliver and Boyd, London, 1961).

81. R.E. Zirkle, Some effects of alpha radiation upon plant cells, J. Cell. Comp. Physiol. 2, 251 (1932).

82. R.E. Zirkle and W. Bloom, Irradiation of parts of individual cells. Science 117, 487 (1953).

83. R.E. Zirkle and C.A. Tobias, Effects of ploidy and energy transfer on radiobiological survival curves, Arch. Biochem. and Biophys. 47, 282 (1953).

84. E.J. Hall (private communication)

85. C.L. Wingate and J.W. Baum (private communication)

TECHNICAL INFORMATION DIVISION
LAWRENCE BERKELEY LABORATORY
UNIVERSITY OF CALIFORNIA
BERKELEY, CALIFORNIA 94720